Design of Floor Crane

Christopher Jin

Professor Sai Cheong Fok

Mechanical Design 1

20 Nov. 2020

Content

1 Introduction ... 1
1.1 History of Floor Cranes ... 1
1.2 Modern Application of Floor Cranes ... 2
2 Preparation for Design ... 3
2.1 Morphology of Design ... 3
2.2 Design Objective and Requirements ... 4
2.2.1 General Objective ... 4
2.2.2 Requirements ... 5
2.3 Material Selection ... 7
2.3.1 Typical Chemical Properties ... 7
2.3.2 Typical Mechanical Properties ... 7
2.4 Parts and Descriptions of Floor Crane ... 7
2.4.1 Main Body ... 7
2.4.2 Pulleys ... 10
2.4.3 Hook ... 10
2.4.4 Nuts and Bolts ... 10
2.4.5 Wheels ... 11
2.4.6 Cables ... 11
3 Design Process ... 12
3.1 Design Criteria for Floor Cranes ... 12
3.2 First Design for Floor Cranes ... 12
3.3 Second Design for Floor Cranes ... 17
3.4 Third Design for Floor Cranes ... 23
3.5 Fourth (Final) Design for Floor Cranes ... 31
4 Analysis for Design of Floor Cranes ... 38
4.1 Floor Load Analysis ... 38
4.2 Main Body Analysis ... 38
4.2.1 Horizontal Arm Analysis ... 39
4.2.2 Vertical Column Analysis ... 45
4.2.3 Base Analysis ... 47

4.3 Hook Analysis 47
4.3.1 Hook Stress Analysis 48
4.3.2 Hook Deflection Analysis 49
4.4 Cable Analysis 50
5 Evaluation of Cost 51
5.1 Cost of Rectangular Tube 51
5.2 Cost of Hook 51
5.3 Cost of Wheels 51
5.4 Cost of Pulleys and Cable 52
5.5 Total Cost 52
6 Conclusion 53
Reference 54

Design of Floor Crane

1 Introduction

1.1 History of Floor Cranes

For thousands of years, people have used innovative ways of lifting really heavy objects and bringing them where they are needed. As demonstrated at Stonehenge, the Pyramids of Giza, and countless ancient sites around the world, the history of the crane is closely aligned with the history of the limits of man's strength.

The birth of the crane is inextricably tied with the birth of the pulley — first devised by ancient Mesopotamians as early as 1500 BC for hoisting water. The first compound pulleys were created by Archimedes of Syracuse around 287 – 212 BC, which he used to lift an entire warship, along with its crew. [1]

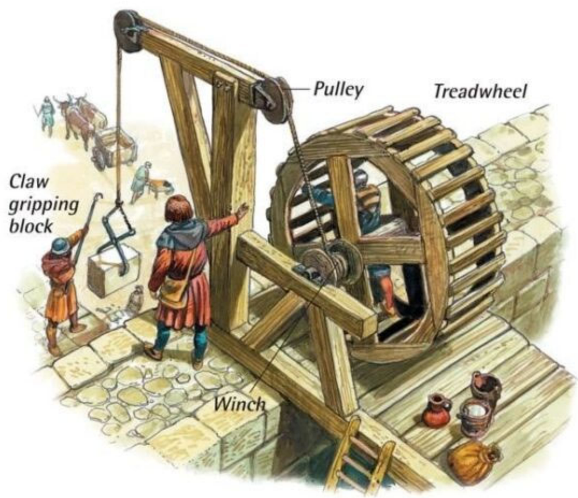

FIGURE 1 THE STRUCTURE OF ANCIENT CRANE

The ancient cranes have been evolving from the load prop to perform various tasks. There are ancient documents where the use of machines similar to cranes by the Sumerians and Chaldeans is evidenced, transmitting this knowledge to the Egyptians. The modern hydraulic crane was invented in Newcastle by William Armstrong in about 1845 to help load coal into barges at the Quayside.

FIGURE 2 ANCIENT CRANE

1.2 Modern Application of Floor Cranes

Nowadays, floor cranes provide an efficient, low cost alternative to other material handling equipment. Strong, robust, sturdy, and built to very standard, these cranes are maneuverable in loading, unloading, and shifting of heavy loads. A portable floor crane is designed for hoisting and transporting materials quickly and safely in different factory and warehouse environments. Units consist of a durable support structure made of welded steel, which ensures a long service life. Crane structure consists of chassis, vertical column, horizontal arm, and the lifting system. The box crane can take heavy loads effectively, avoids damage under rough and unskilled handling.

Cranes exist in an enormous variety of forms—each tailored to a specific use. Sometimes sizes range from the smallest jib cranes, used inside workshops, to the tallest tower cranes, used for constructing high buildings. For a while, mini-cranes are also used for constructing high buildings, in order to facilitate constructions by reaching tight spaces. Finally, we can find larger floating cranes, generally used to build oil rigs and salvage sunken ships.

FIGURE 3 TYPICAL FLOOR CRANES

The primary purpose of this project is to present the design procedure of the floor cranes. The discussion will start with a design objective and a set of design requirements. These items are followed by design of each part. The emphasis is placed on the selection of the structural components and the welds. There is more than one solution to any design problem; therefore, the selections in this chapter are not unique. The calculations are for a prototype machine that should be evaluated in the laboratory.

2 Preparation for Design

2.1 Morphology of Design

In designing a machine component, there is no rigid rule. The problem may be attempted in several ways. However, the general procedure to solve a design problem is as follows:

1. Recognition of need: First of all, make a complete statement of the problem, indicating the need, aim or purpose for which the machine is to be designed.
2. Synthesis (mechanisms): Select the possible mechanism or group of mechanism, which will give the desired motion.
3. Analysis of forces: Find the forces acting on each member of the machine and the energy transmitted by each member.
4. Material selection: Select the appropriate material suited for each member of the machine best.
5. Design of elements (size and stresses): Find the size of each member of the machine by considering the forces acting on the member and the permissible stresses for the material used. It should be kept in mind that each member should not deflector deform than the permissible limit.
6. Modification: Modify the size of the member to agree with the past experience and judgment to facilitate manufacture. The modification may also be necessary by considering of manufacturing to reduce overall cost.
7. Detailed drawing: Draw the detailed of each component and the assembly of the machine with complete specification for the manufacturing process suggested.
8. Production: The component, as per the drawing, is manufactured in the workshop.

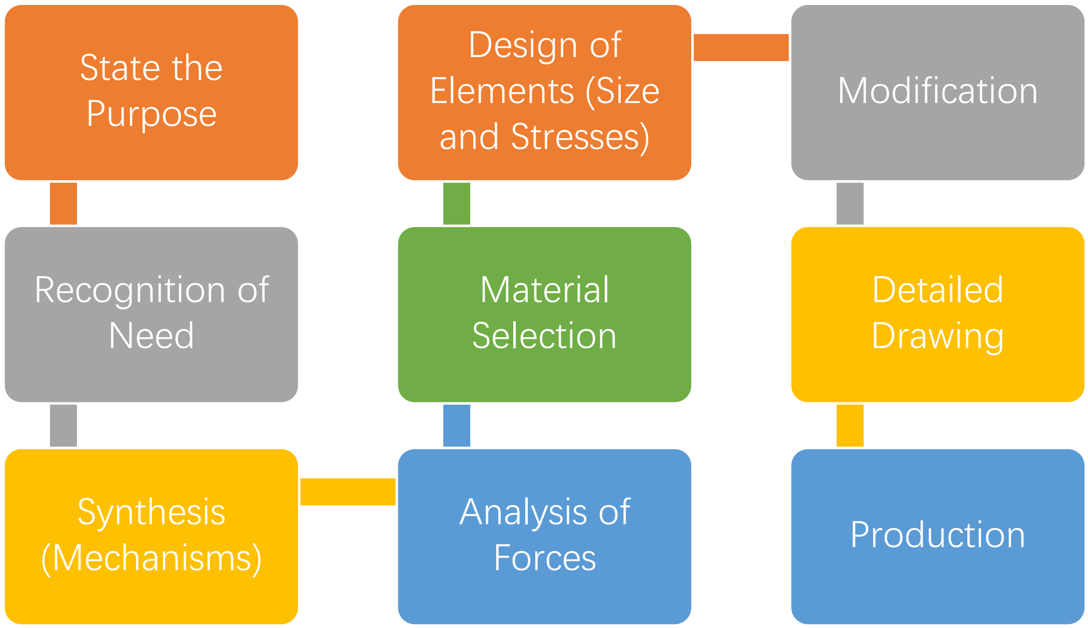

FIGURE 4 MORPHOLOGY OF DESIGN

2.2 Design Objective and Requirements

Every design starts with a general objective and a set of requirements. The general configuration is usually known but many of the final dimensions need to be determined. The final product must fit together, which means providing the appropriate clearance for moving pieces and having enough space for the fillet welds. The design objective and requirements are often accompanied by a short commentary that explains the reason for some of the requirements.

2.2.1 GENERAL OBJECTIVE

Specify a set of structural components and the appropriate welds for the floor crane shown in Figure below. The crane has a permanent shape and supports a maximum load of 400 kg.

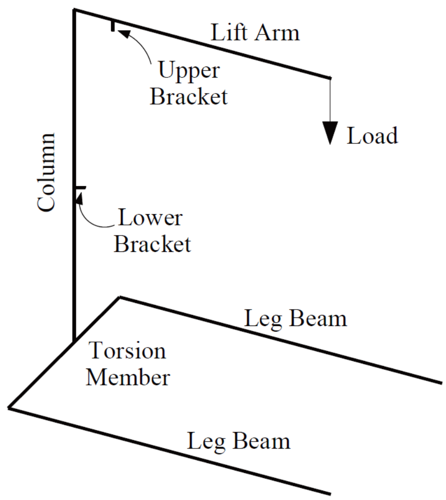

FIGURE 5 SKETCH OF FLOOR CRANES

2.2.2 REQUIREMENTS

1. The lift arm has a length of 1200 mm. The centerline of the upper bracket is 80 mm from the pin that attaches the lift arm to the column. The column has a length of 1600 mm with the centerline location of the lower bracket to be determined.
2. The members in the plane grid have the centerline dimensions shown in figure below. The crane has fixed wheels at the ends of the leg beams and swivel wheels at the end of the torsion member. The centerline of the wheels on each leg beam shall be at the 1600 mm dimension. The centerline distance between the two leg beams is 1000 mm.
3. The primary structural components shall be made from square or rectangular structural tubes. The components shall be design using the noncompact design criteria where appropriate. The structural members can be either ASTM 501 or ASTM A500, Grade B steel.
4. The column shall be attached to the torsion member by a fillet weld that goes completely around the column.
5. The torsion member shall be attached to the side of each leg beam by a fillet weld that goes completely around the torsion member.
6. The upper and lower brackets shall be identical pieces with identical welds.

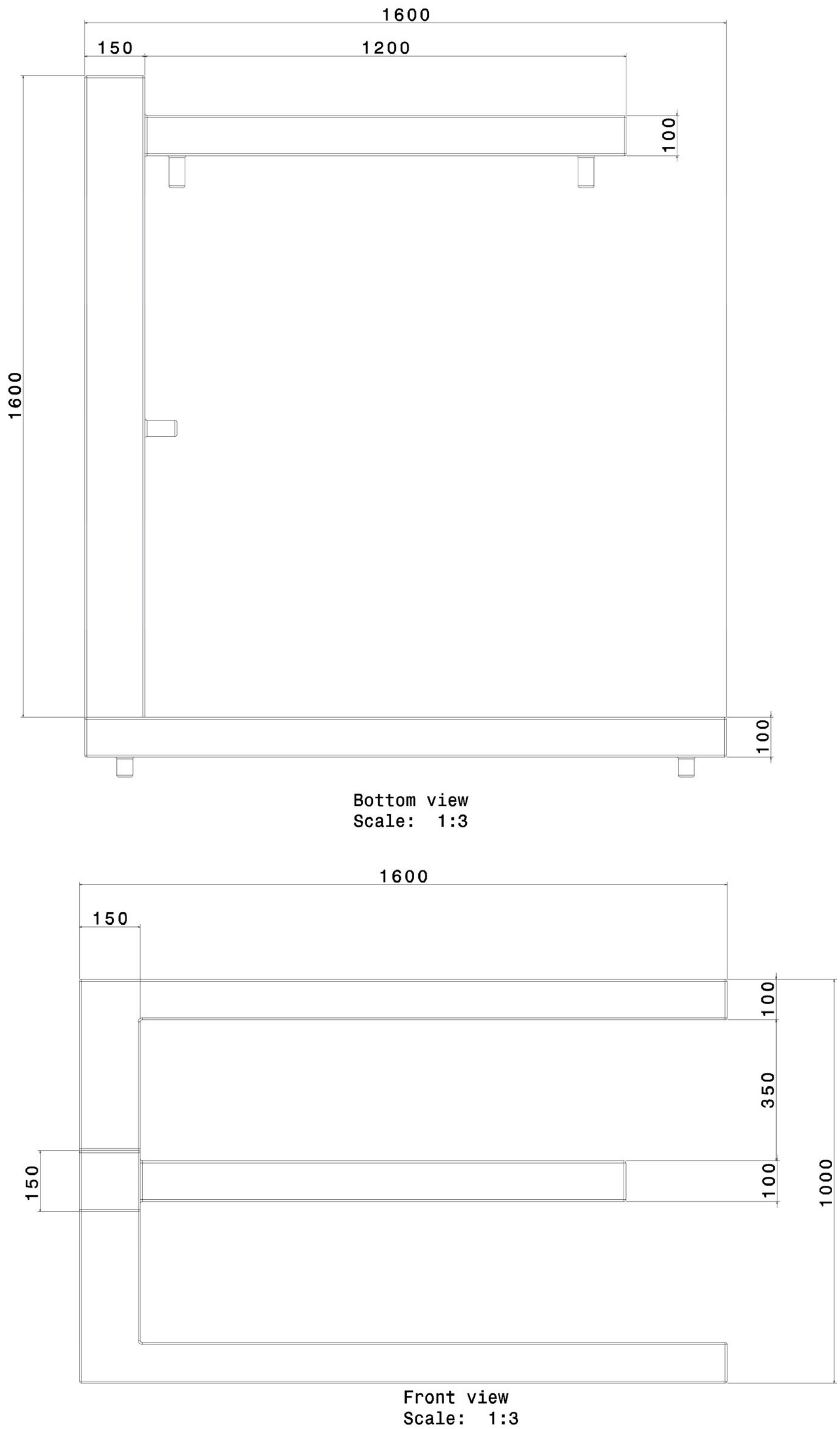

FIGURE 6 DIMENSION AND OTHER REQUIREMENTS FOR THE FLOOR CRANE.

2.3 Material Selection

In this project, I select ASTM A500, Grade B steel as structural members. ASTM A500 is a standard specification for cold-formed welded and seamless carbon steel structural tubing in round, square and rectangular shapes. I choose this material because it is easy to weld, cut, form and machine. It is widely used in frames, roll cages, truck racks, trailers, railings, etc.

2.3.1 Typical Chemical Properties

Table 1 Typical Chemical Properties

Structural Tube	Grades A, B, and D		Grade C	
	Heat analysis	Product analysis	Heat analysis	Product analysis
Carbon, %	0.26	0.3	0.23	0.27
Manganese, %	1.35	1.4	1.35	1.4
Phosphorous, %	0.035	0.045	0.035	0.045
Sulfur, %	0.035	0.045	0.035	0.045
Copper, %	0.2	0.18	0.2	0.18

2.3.2 Typical Mechanical Properties

Table 2 Typical Mechanical Properties

Structural Tube	Grade A	Grade B	Grade C	Grade D
Tensile Strength, psi [Mpa]	45,000 [310]	58,000 [400]	62,000 [425]	58,000 [400]
Yield Strength, psi [Mpa]	39,000 [270]	46,000 [315]	50,000 [345]	36,000 [250]

2.4 Parts and Descriptions of Floor Crane

2.4.1 Main Body

The main body contains three parts: the base plate, the vertical column, and the horizontal arm, as shown in figure below.

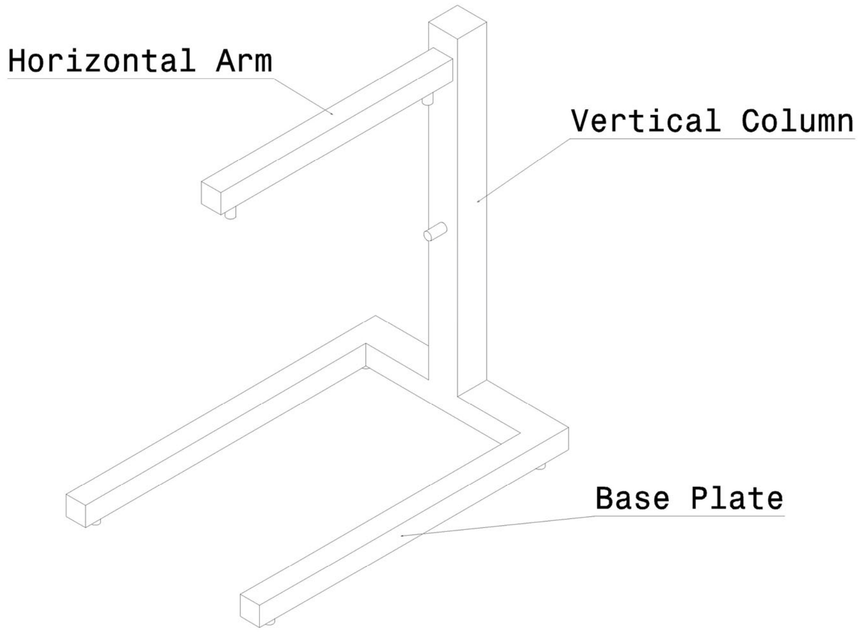

FIGURE 7 MAIN BODY

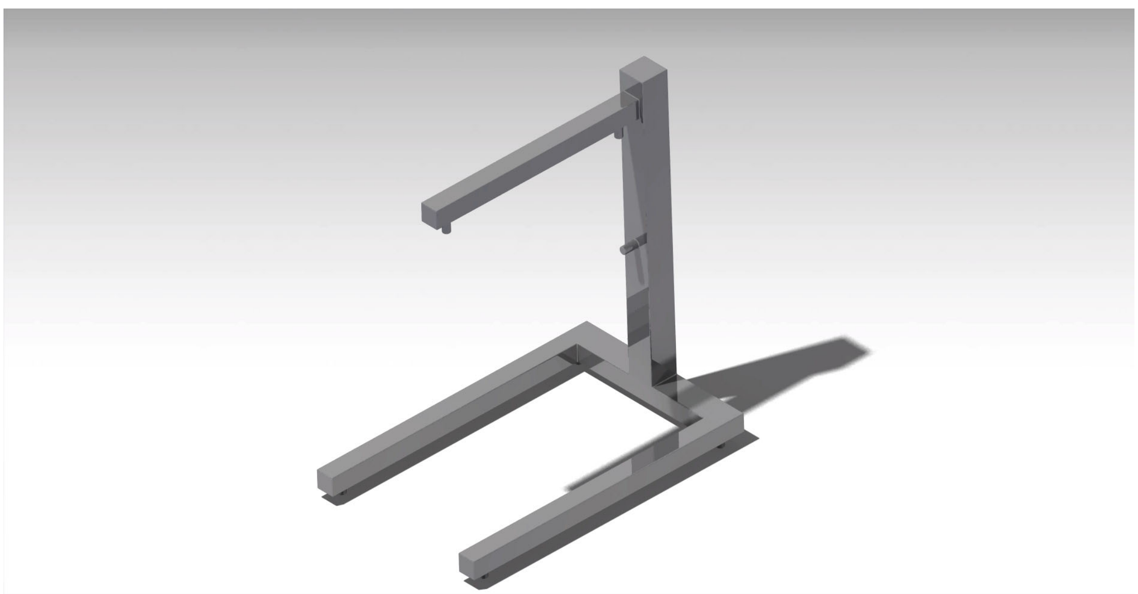

FIGURE 8 3D MAIN BODY

2.4.1.1 BASE PLATE

The base plate is a plate that serves as a base or support. The base is the load-bearing part of the entire floor crane. Generally speaking, the structure of the base determines the stability of the entire machine.

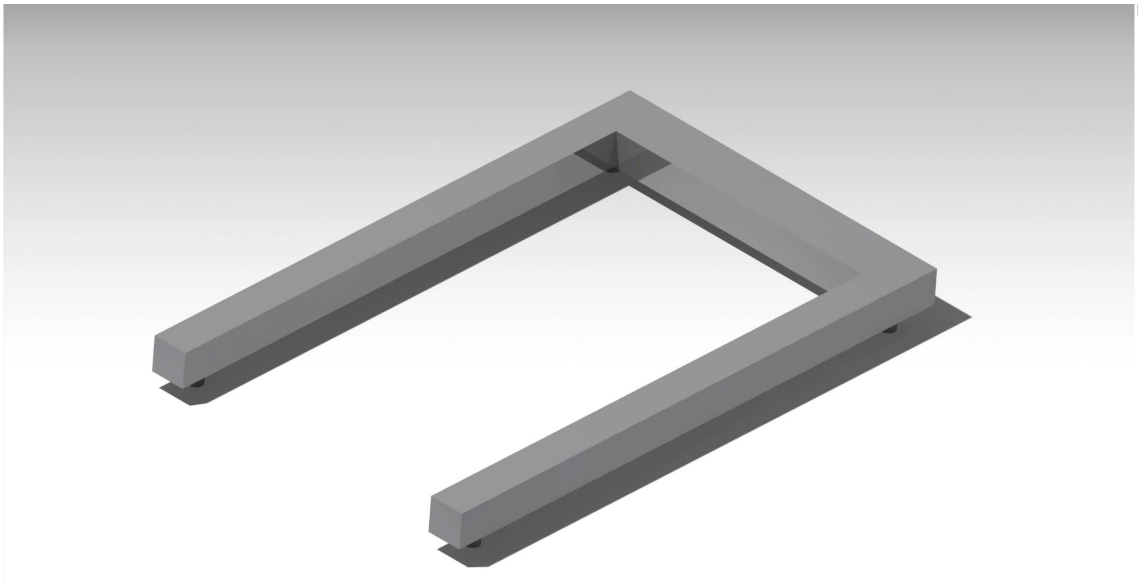

FIGURE 9 BASE PLATE

The 3D view and the dimensions of the base plate of the floor crane are shown in figure below:

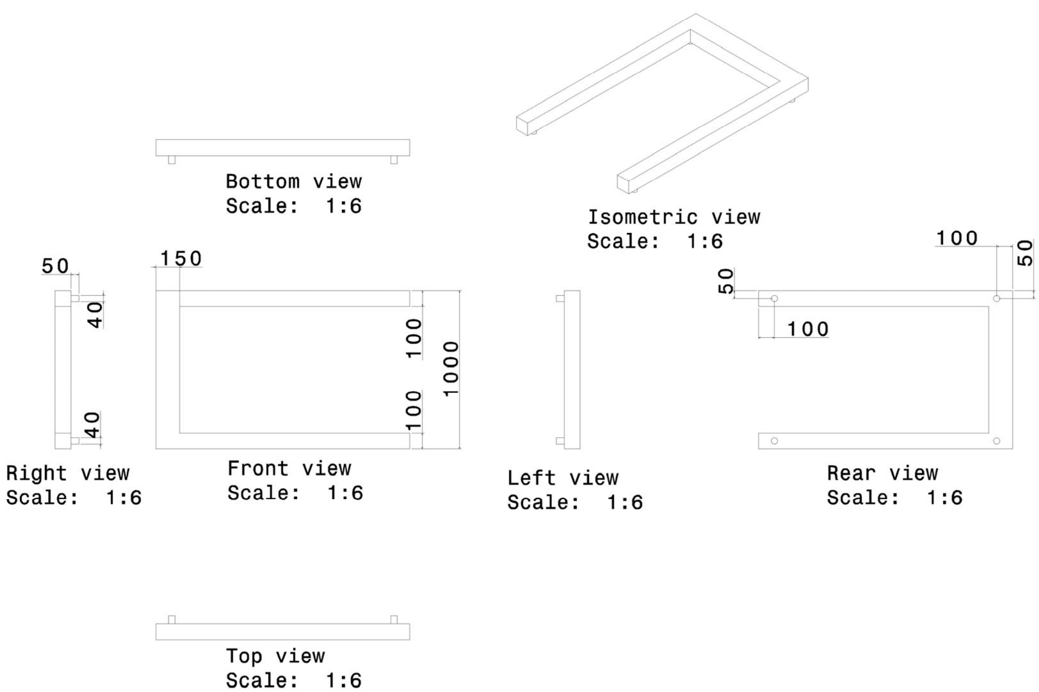

FIGURE 10 3D VIEW OF BASE

2.4.1.2 HORIZONTAL ARM

It is fixed horizontal arm on which our pulleys are mounted. It is fixed with the vertical column with welded joint.

2.4.1.3 VERTICAL COLUMN

This is mounted on the pallet/base plate/truck in longitudinal or y-direction.

2.4.2 PULLEYS

A pulley is a wheel on an axle that is designed to support movement and change of direction of a cable or belt along its circumference. Pulleys are used in a variety of ways to lift loads, apply forces, and to transmit power. A pulley is also called a sheave or drum and may have a groove between two flanges around its circumference. The drive element of a pulley system can be a cable, cable, belt, or chain that runs over the pulley inside the groove.

FIGURE 11 PULLEYS

2.4.3 HOOK

Hook is fixed with the cables moving on pulleys. Hook is used for attaching the load to horizontal arm which moves up and down due which the connected loads are lifted and rotates.

FIGURE 12 HOOK

2.4.4 NUTS AND BOLTS

Nuts and bolts are the hardware fasteners which are used to fasten the various different parts.

FIGURE 13 NUTS AND BOLTS

2.4.5 WHEELS

A wheel is a circular component that is intended to rotate on an axial bearing. The wheel is one of the main components of the wheel and axle which is one of the six simple machines. Wheels, in conjunction with axles, allow heavy objects to be moved easily facilitating movement or transportation while supporting a load, or performing labor in machines. In my project, I am using four wheels of diameter 80 mm.

FIGURE 14 WHEELS

2.4.6 CABLES

Cables are used in the lifting system of the floor cranes. Because we have to lift very heavy objects, we have high requirements for cables.

FIGURE 15 CABLES

3 Design Process

3.1 Design Criteria for Floor Cranes

There are three major considerations in the design of cranes.

1. The floor crane must be able to lift the weight of the load.
2. The floor crane must not rupture.
3. The floor crane must not topple.

3.2 First Design for Floor Cranes

I designed a solid Floor Crane with ASTM A500, Grade B steel based on the previous sketch, which is shown in figure below.

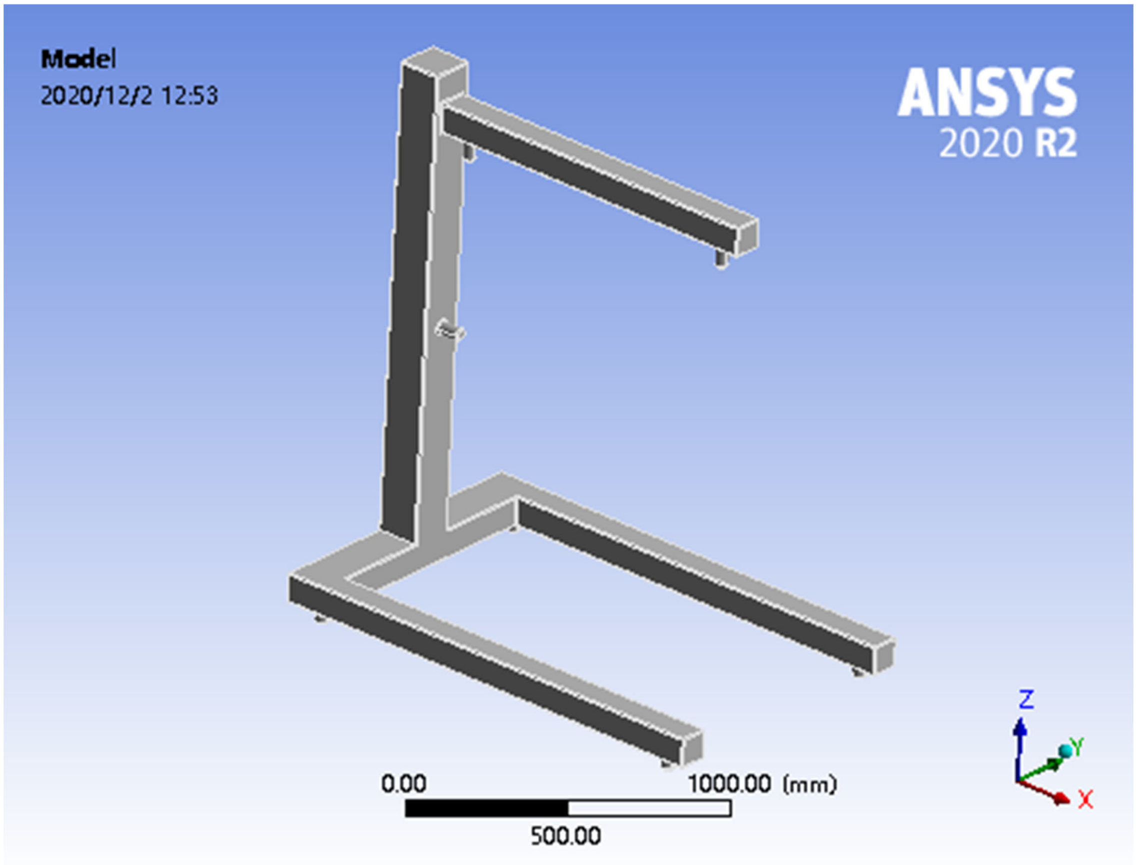

FIGURE 16 FIRST DESIGN OF FLOOR CRANES

However, from the data in ANSYS, I find that the mass of the first design is too high, which is 725.37 kg, as shown in tables below.

TABLE 3 BOUNDING BOX OF FIRST DESIGN OF FLOOR CRANES

Bounding Box	
Length X	1600. mm
Length Y	1000. mm
Length Z	1750. mm

TABLE 4 PROPERTIES OF FIRST DESIGN OF FLOOR CRANES

Properties	
Volume	9.2404e+007 mm³
Mass	725.37 kg
Centroid X	416.45 mm
Centroid Y	6.0783e-004 mm
Centroid Z	578.87 mm
Moment of Inertia Ip1	3.4298e+008 kg·mm²
Moment of Inertia Ip2	4.352e+008 kg·mm²
Moment of Inertia Ip3	2.0617e+008 kg·mm²

Christopher King

And then, I check the mechanics behavior of the first design to determine whether this design direction is correct. Here are the figures for analysis from ANSYS.

TABLE 5 TOTAL DEFORMATION OF FIRST DESIGN OF FLOOR CRANES

Time [s]	Minimum [mm]	Maximum [mm]	Average [mm]
1.	0.	4.5456	1.7954

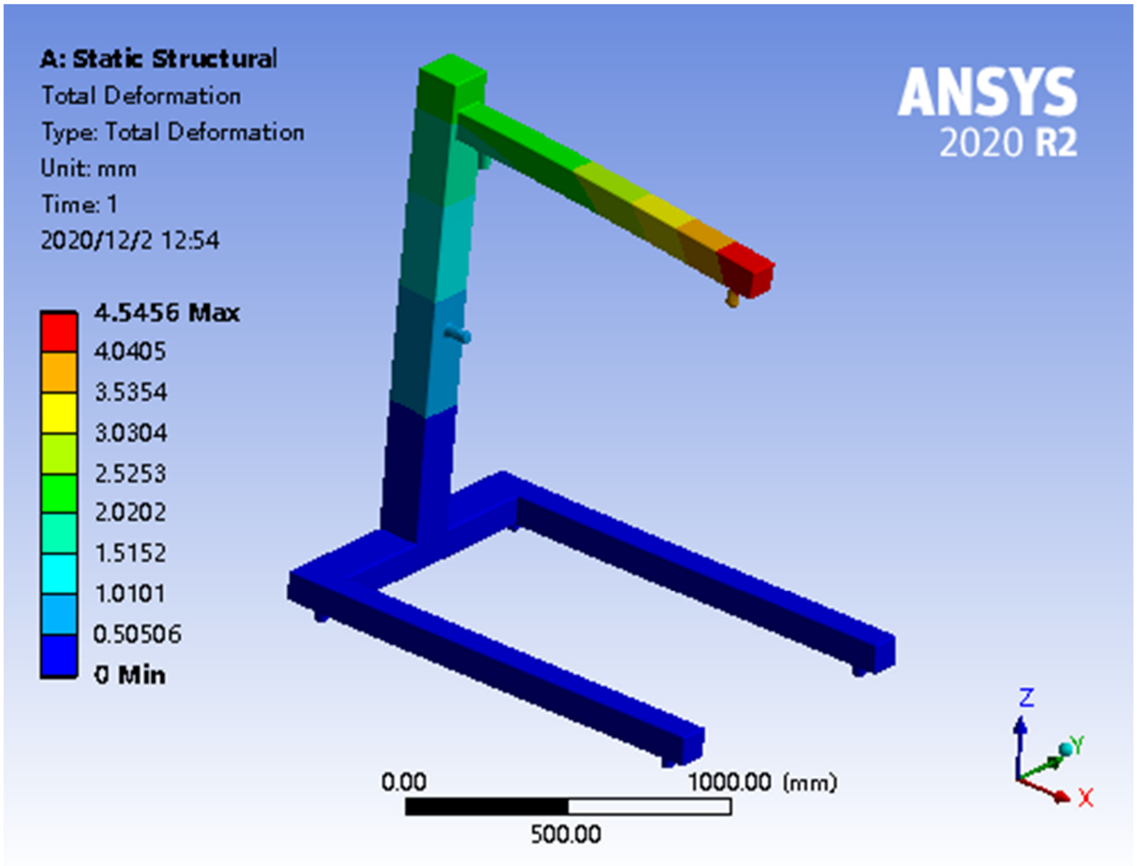

FIGURE 17 TOTAL DEFORMATION OF FIRST DESIGN OF FLOOR CRANES

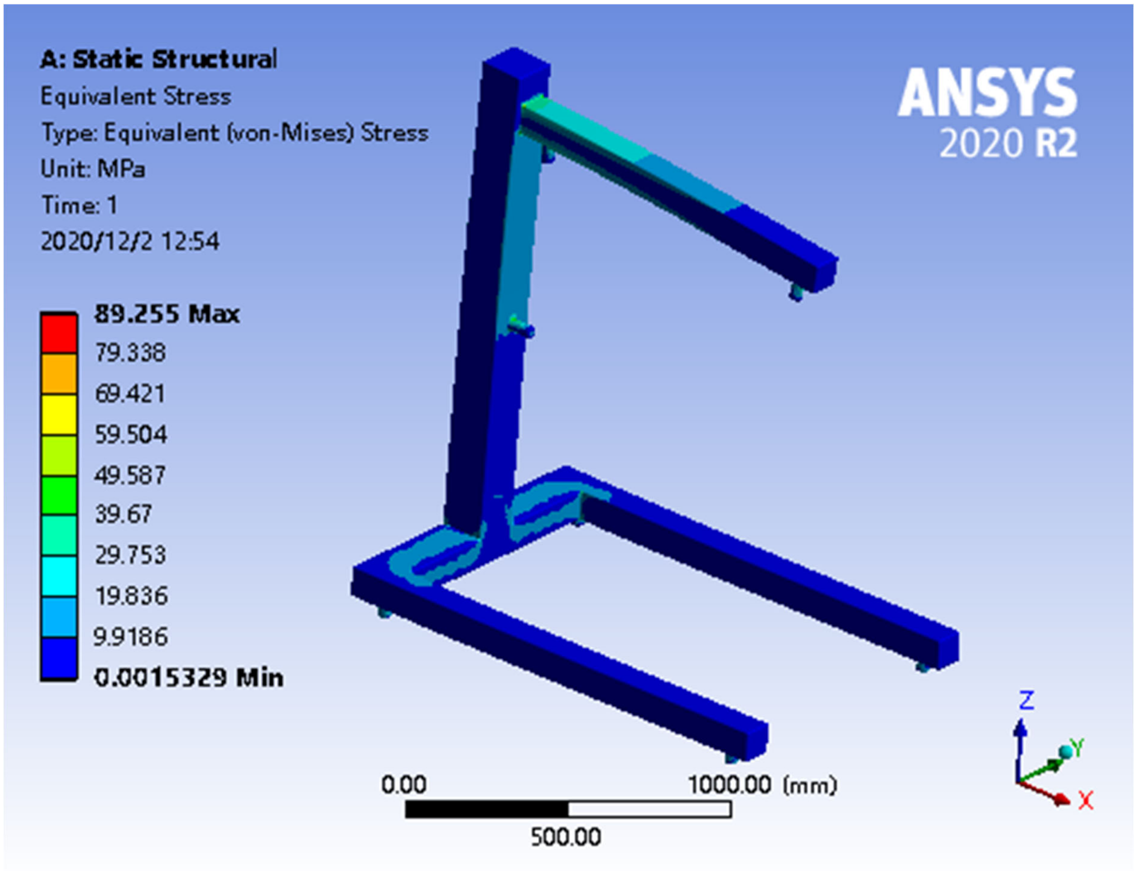

FIGURE 18 EQUIVALENT STRESS OF FIRST DESIGN OF FLOOR CRANES

TABLE 6 EQUIVALENT STRESS OF FIRST DESIGN OF FLOOR CRANES

Time [s]	Minimum [MPa]	Maximum [MPa]	Average [MPa]
1.	1.5329e-003	89.255	11.301

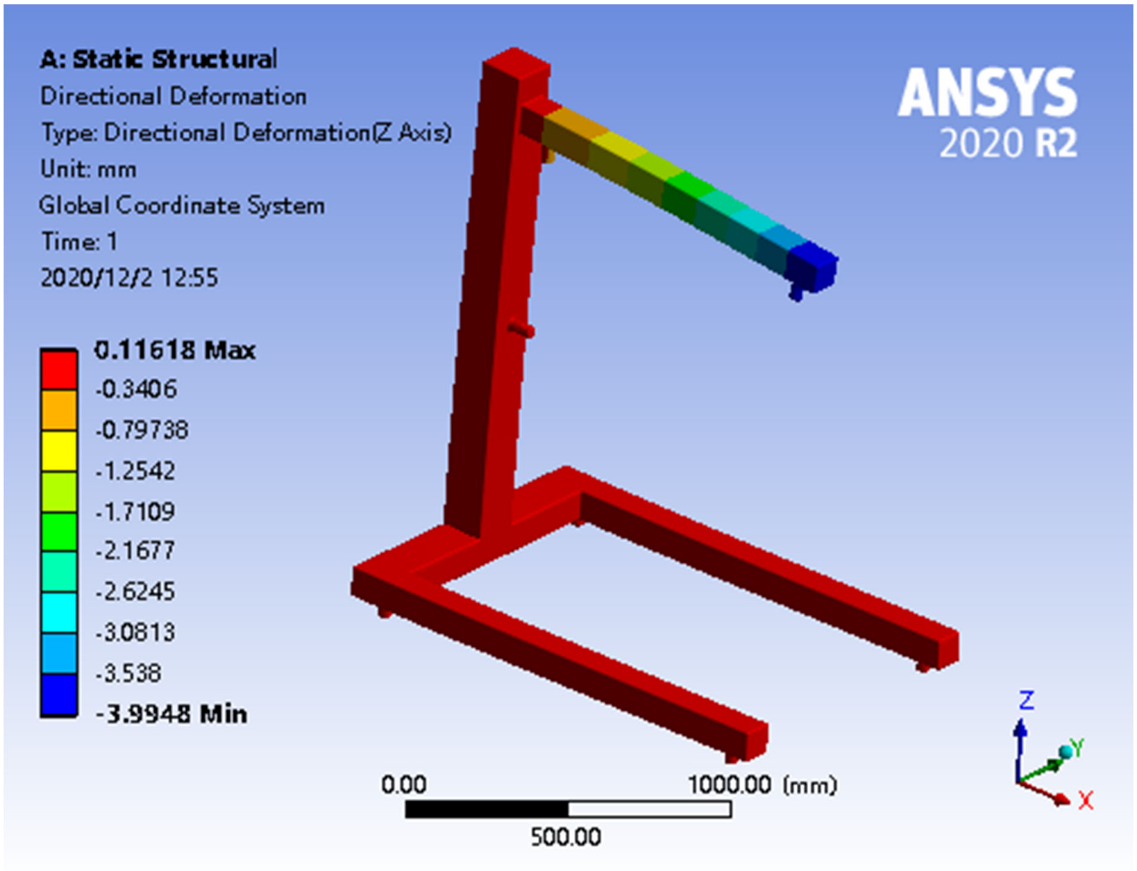

FIGURE 19 DIRECTIONAL DEFORMATION OF FIRST DESIGN OF FLOOR CRANES

TABLE 7 DIRECTIONAL DEFORMATION OF FIRST DESIGN OF FLOOR CRANES

Time [s]	Minimum [mm]	Maximum [mm]	Average [mm]
1.	-3.9948	0.11618	-1.0745

From the analysis results shown in figures and tables above, I can know that although the mass of the first design is too large, the mechanics behavior of it is pretty good, because the maximum equivalent stress is only 89.255 MPa. Therefore, the factor of safety for this design can be $FS = \frac{315\ \text{MPa}}{89.255\ \text{MPa}} = 3.5$, which is very safe.

The second thing I can know from the equivalent stress figure is that the maximum equivalent stress occurs at the location shown below:

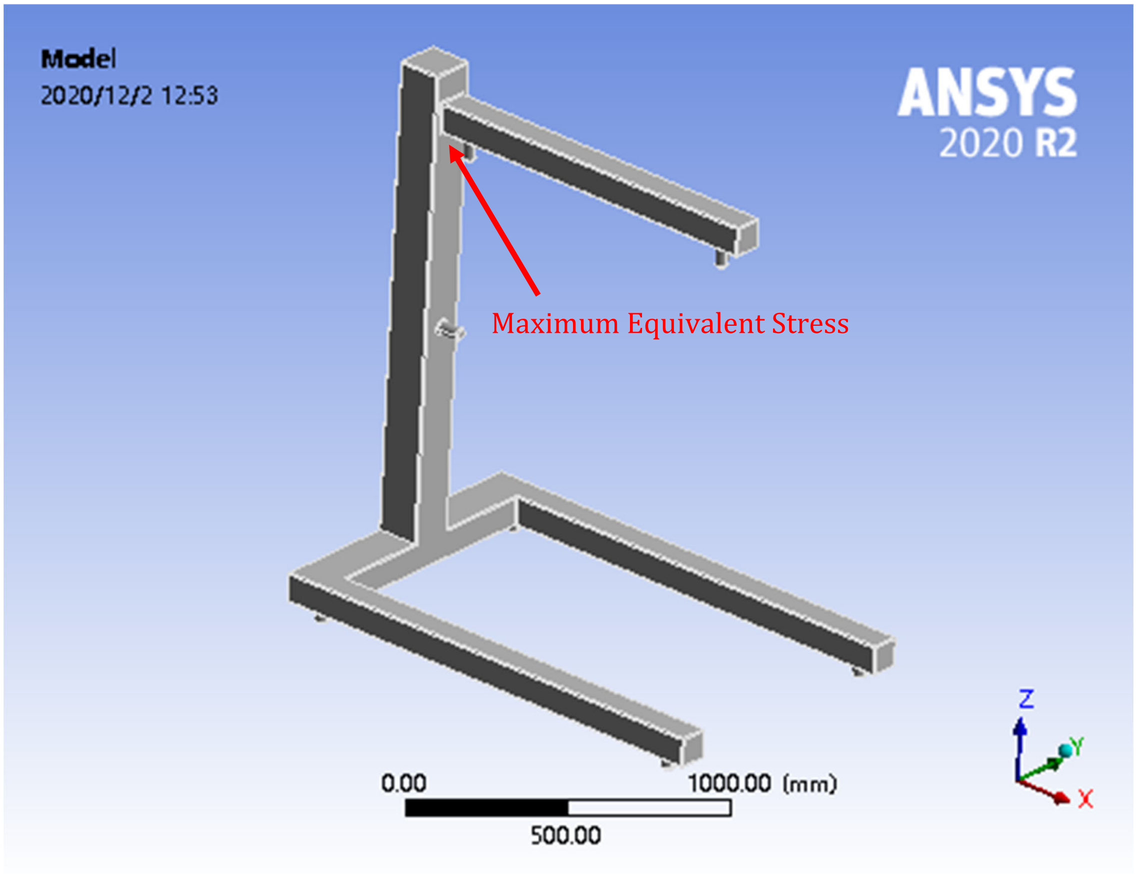

FIGURE 20 LOCATION OF MAXIMUM EQUIVALENT STRESS

However, in this design, I find that the stress concentration is not large, which is only about 1.4. Therefore, I do not change the shape near where the maximum equivalent stress occurs during my second design.

The third thing I notice is that the maximum total deformation of the first design of the floor crane is about 4.5456 mm, which is quite small compared to the total length of the horizontal arm, which is equal to 1200 mm.

Due to the large mass of the floor crane in the first design, I begin my second design to solve the problem.

3.3 Second Design for Floor Cranes

The problem in my first design is that the mass is too large. Therefore, in this design, I try to reduce the mass of the whole part. In order to do this, one of the ideas is to use the tube instead of the solid bar. Therefore, I replace all the ASTM A500, Grade B steel bar in the first design with ASTM A500, Grade B steel tube, which is shown in figure below.

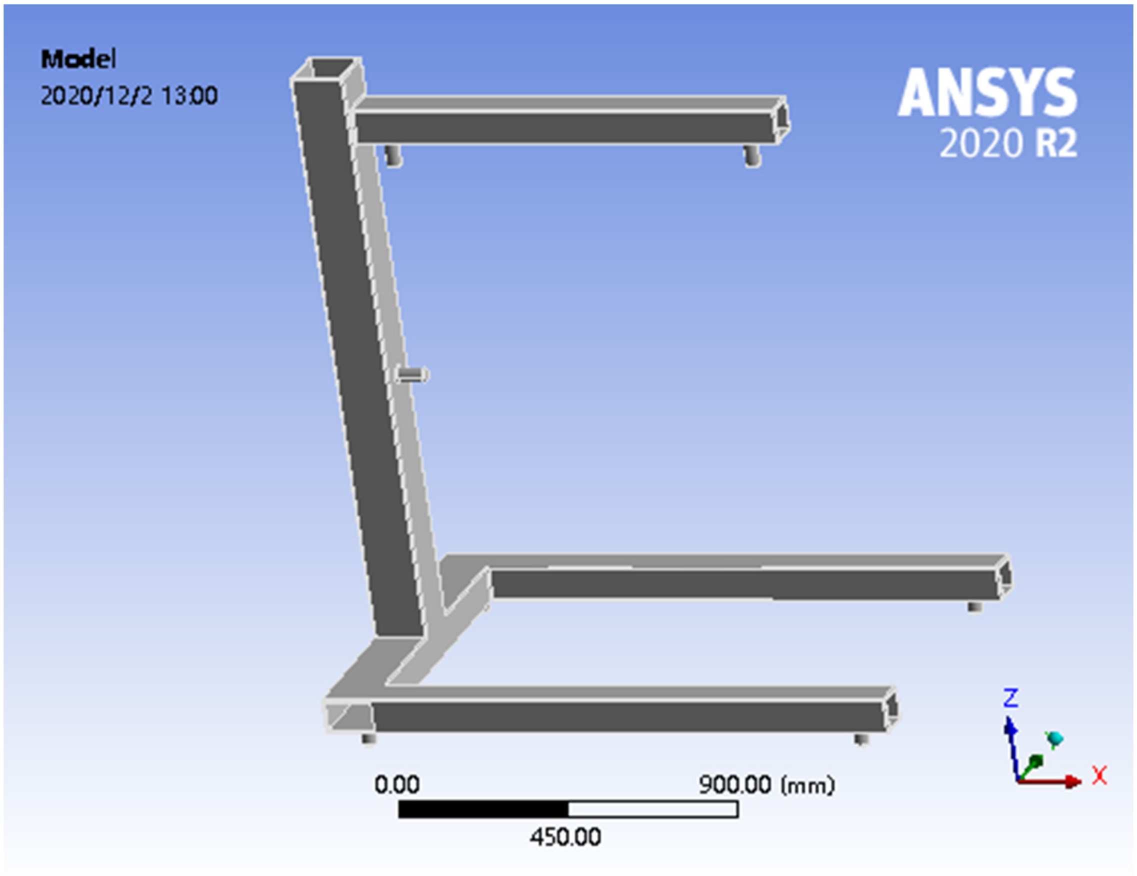

FIGURE 21 SECOND DESIGN OF FLOOR CRANES

From the tables below, I can find that the mass of the whole part has reduced hugely, which means my goal has been achieved by replacing the solid rod with the rectangular tube.

TABLE 8 BOUNDING BOX OF SECOND DESIGN OF FLOOR CRANES

Bounding Box	
Length X	1600. mm
Length Y	1000. mm
Length Z	1750. mm

TABLE 9 PROPERTIES OF SECOND DESIGN OF FLOOR CRANES

Properties	
Volume	2.8724e+007 mm³
Mass	225.48 kg
Centroid X	476.04 mm
Centroid Y	1.9961e-003 mm
Centroid Z	550.13 mm
Moment of Inertia Ip1	1.1148e+008 kg·mm²
Moment of Inertia Ip2	1.4166e+008 kg·mm²
Moment of Inertia Ip3	7.071e+007 kg·mm²

Christopher King

The 3D Sketch and the dimensions of the second design are shown in figure below.

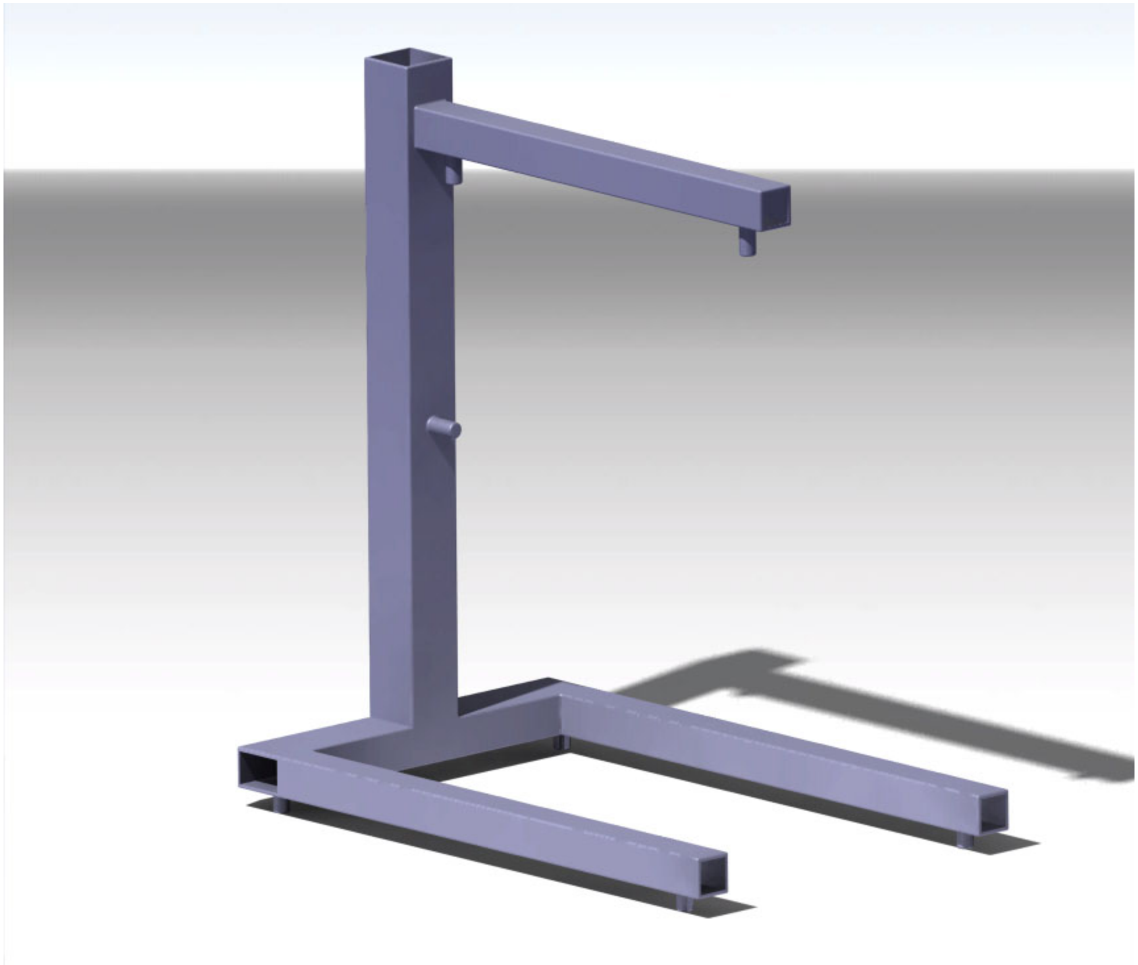

FIGURE 22 3D SKETCH FOR SECOND DESIGN OF FLOOR CRANES

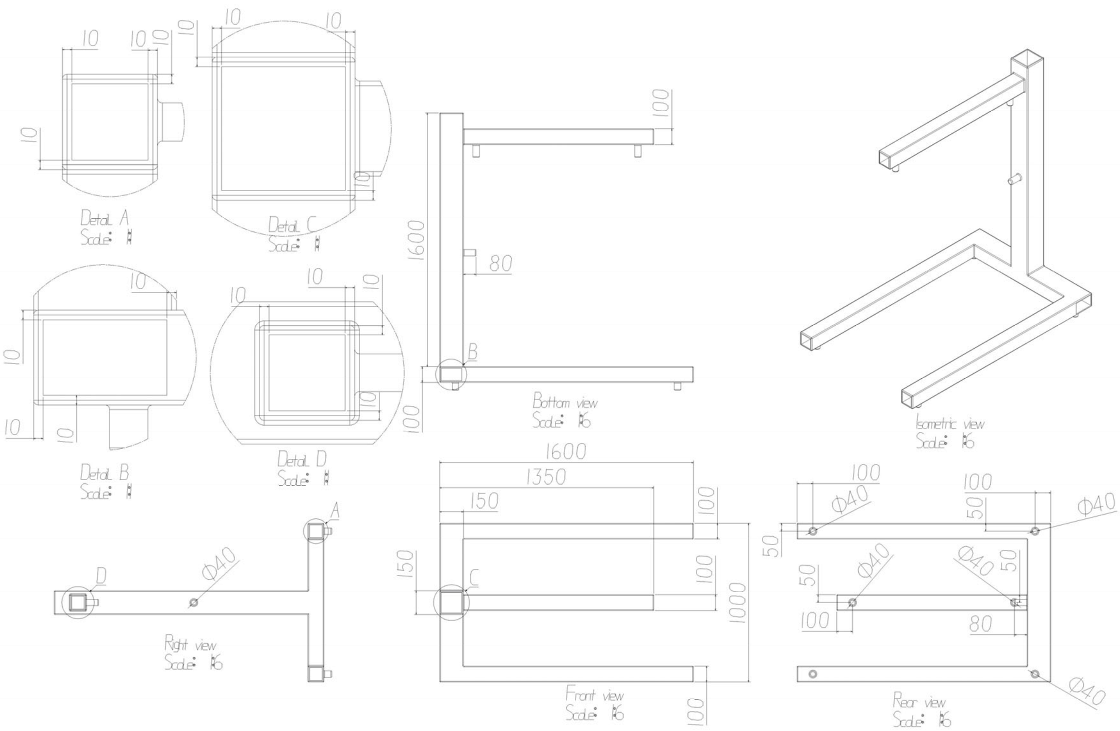

FIGURE 23 DIMENSIONS FOR SECOND DESIGN OF FLOOR CRANES

Next, let me check the mechanics behavior of the second design to determine whether the structure meets the need to support the 400 kg weight. Here are the figures for analysis from ANSYS.

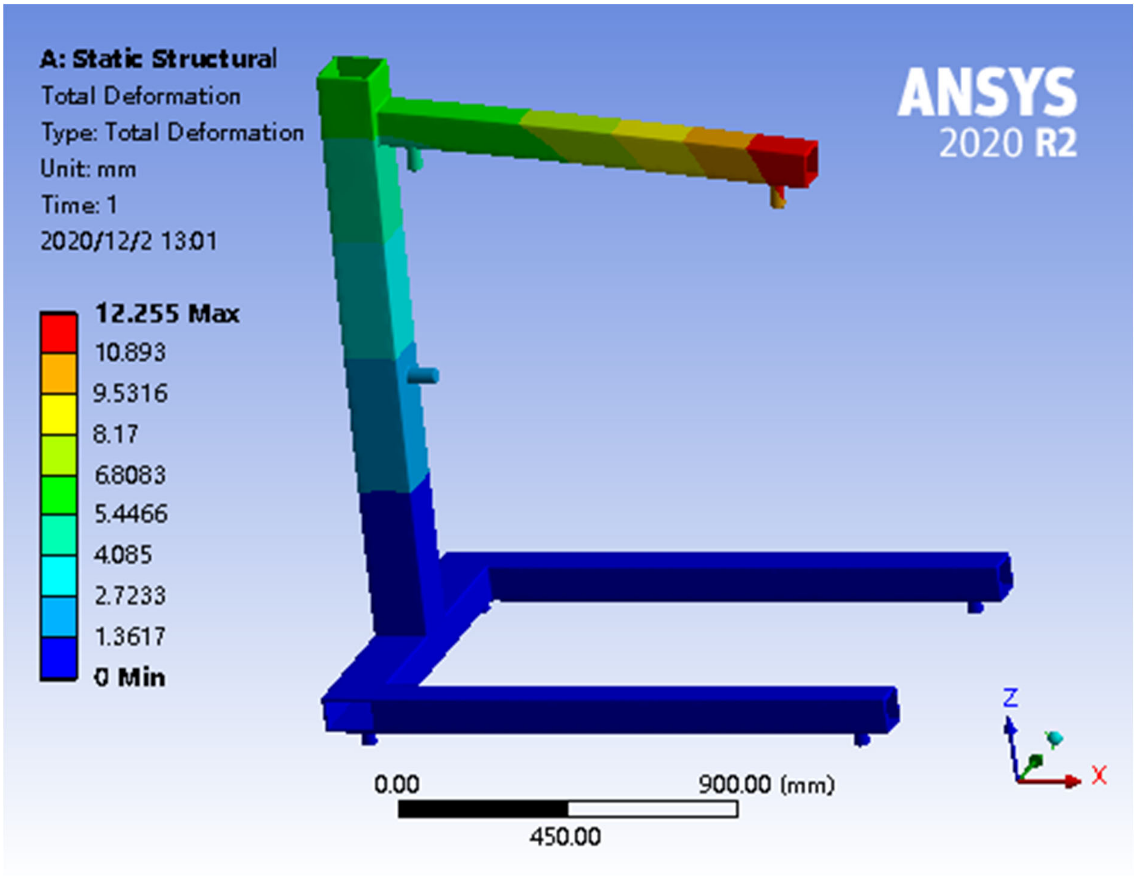

FIGURE 24 TOTAL DEFORMATION OF SECOND DESIGN OF FLOOR CRANES

TABLE 10 TOTAL DEFORMATION OF SECOND DESIGN OF FLOOR CRANES

Time [s]	Minimum [mm]	Maximum [mm]	Average [mm]
1.	0.	12.255	6.6368

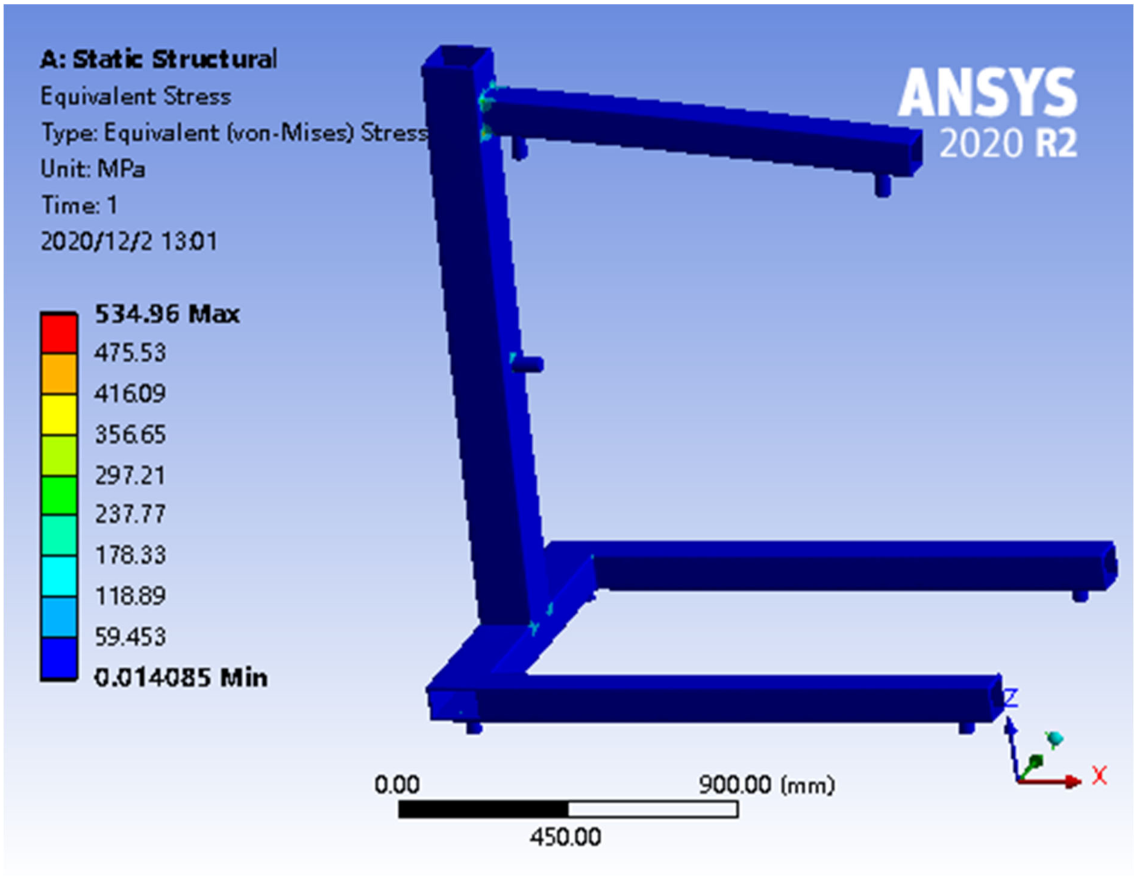

FIGURE 25 EQUIVALENT STRESS OF SECOND DESIGN OF FLOOR CRANES

TABLE 11 EQUIVALENT STRESS OF SECOND DESIGN OF FLOOR CRANES

Time [s]	Minimum [MPa]	Maximum [MPa]	Average [MPa]
1.	1.4085e-003	534.96	25.481

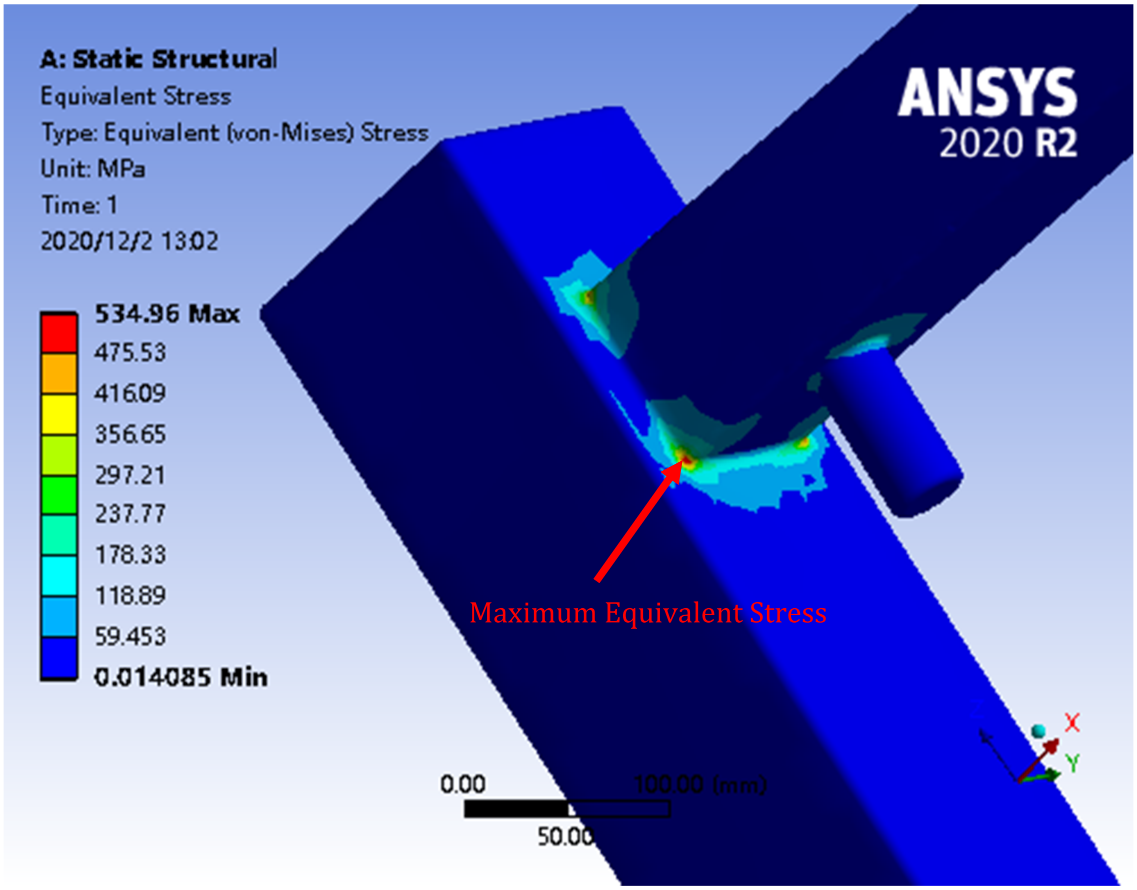

FIGURE 26 ZOOM IN OF EQUIVALENT STRESS OF SECOND DESIGN OF FLOOR CRANES

From the analysis results shown in figures and tables above, I can know that although the problem of large mass has solved, the maximum equivalent stress is too large unfortunately because of the replacement the solid rod with the rectangular, which is 534.96 MPa. This has exceeded the yielding strength of ASTM A500, Grade B steel. Therefore, the second design for the floor cranes has failed.

Besides, from the total deformation figure, I can know that the maximum total deformation of the second design is equal to 12.255 mm, , which is also quite small compared to the total length of the horizontal arm, which is equal to 1200 mm.

Due to the large stress concentration of the floor crane in the second design, I begin my third design to solve the problem.

3.4 Third Design for Floor Cranes

The problem in my second design is that the stress concentration near the intersection between the vertical column and the horizontal arm is too large. Therefore, in this design, I try to reduce the stress concentration . In order to do this, one of the ideas is to add a triangular prism between the vertical column and the horizontal arm, which is shown in figure below.

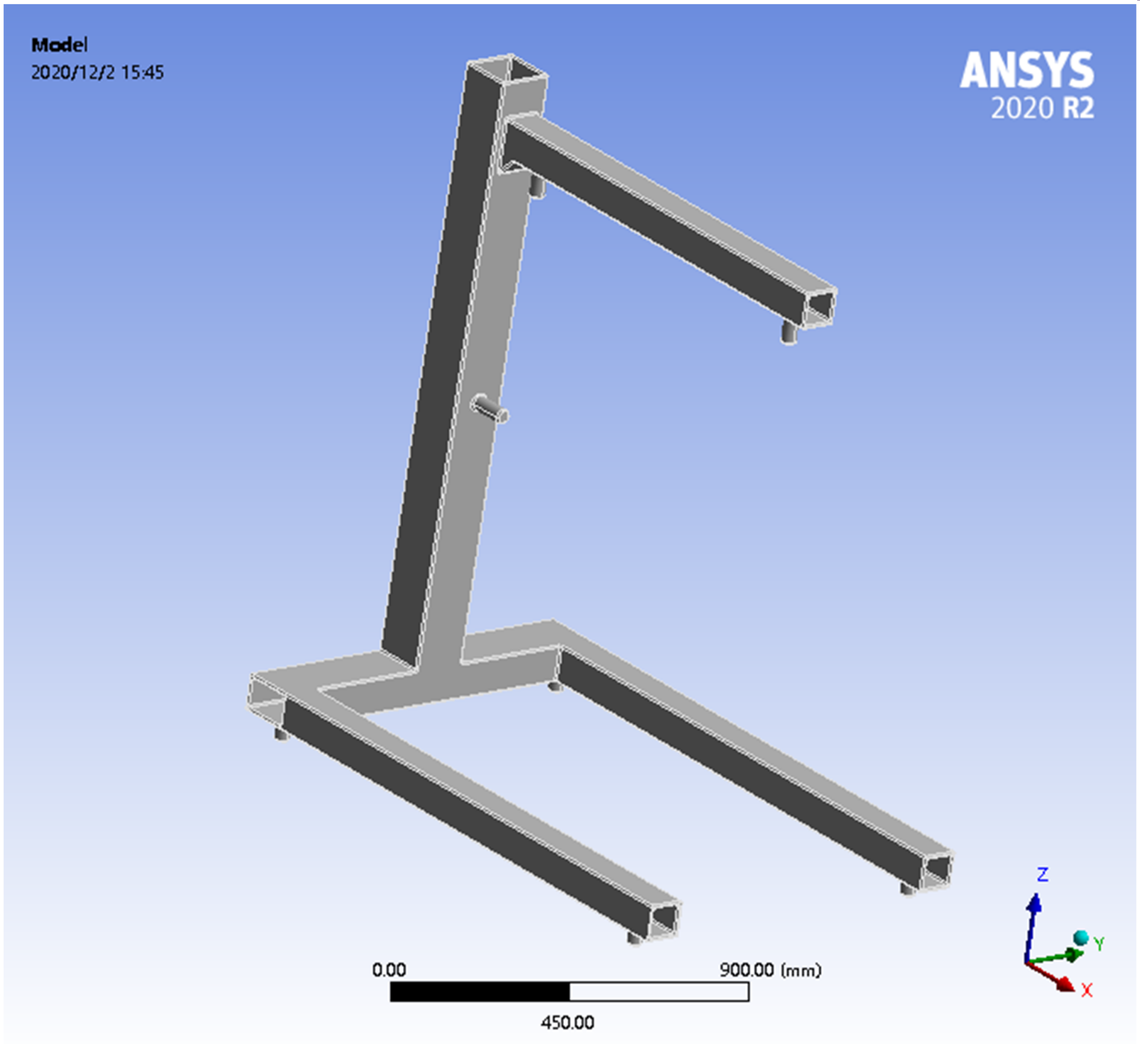

FIGURE 27 THIRD DESIGN OF FLOOR CRANES

From the tables below, I can find that the mass of the whole part is still low relatively.

TABLE 12 BOUNDING BOX OF THIRD DESIGN OF FLOOR CRANES

Bounding Box	
Length X	1600. mm
Length Y	1000. mm
Length Z	1750. mm

TABLE 13 PROPERTIES OF THIRD DESIGN OF FLOOR CRANES

Properties	
Volume	2.9015e+007 mm³
Mass	227.77 kg
Centroid X	474.76 mm
Centroid Y	-1.6396e-002 mm

Centroid Z	554.12 mm
Moment of Inertia Ip1	1.1298e+008 kg·mm²
Moment of Inertia Ip2	1.433e+008 kg·mm²
Moment of Inertia Ip3	7.1068e+007 kg·mm²

The 3D Sketch and the dimensions of the second design are shown in figure below.

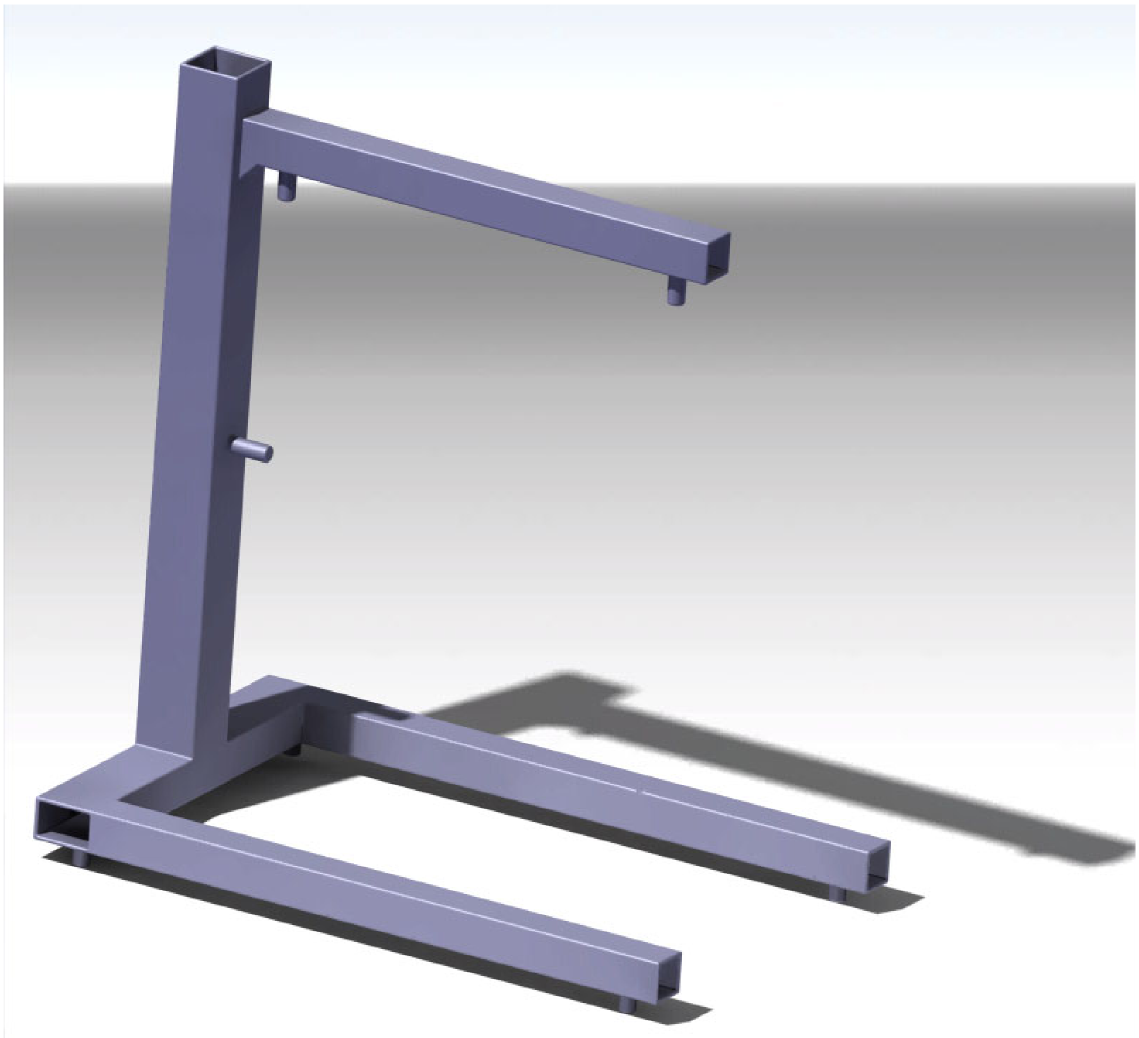

FIGURE 28 SKETCH FOR THIRD DESIGN OF FLOOR CRANES

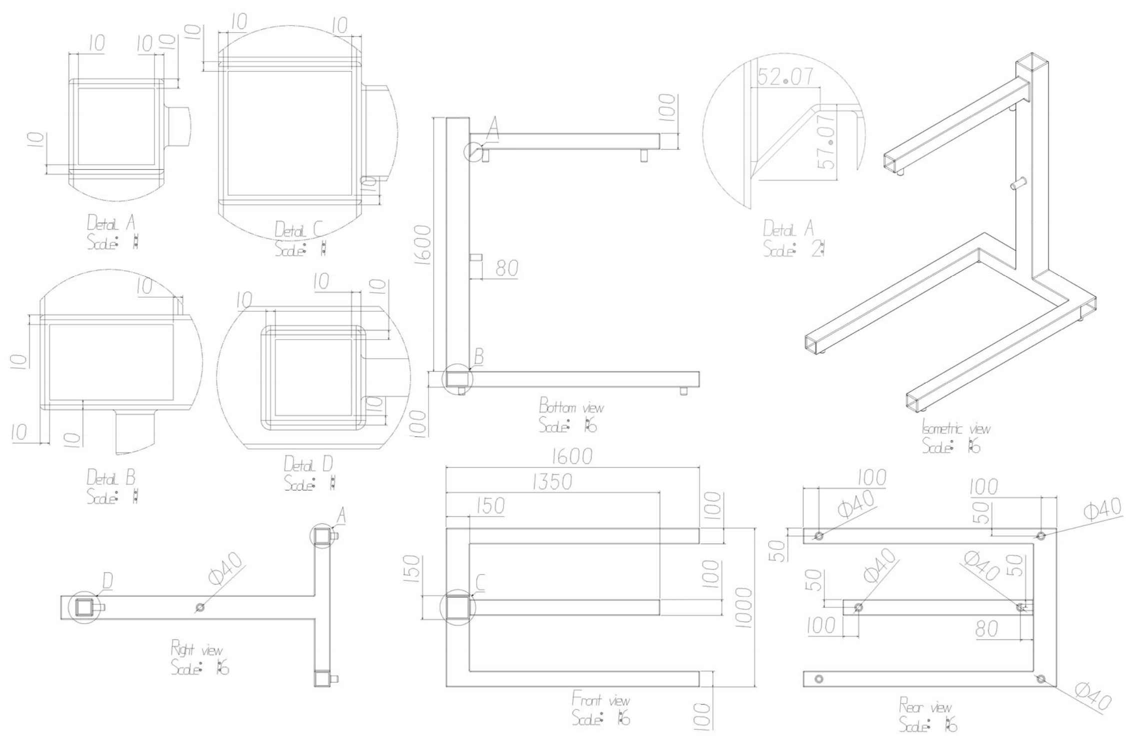

FIGURE 29 DIMENSIONS FOR THIRD DESIGN OF FLOOR CRANES

Next, let me check the mechanics behavior of the third design to determine whether the structure meets the need to support the 400 kg weight. Here are the figures for analysis from ANSYS.

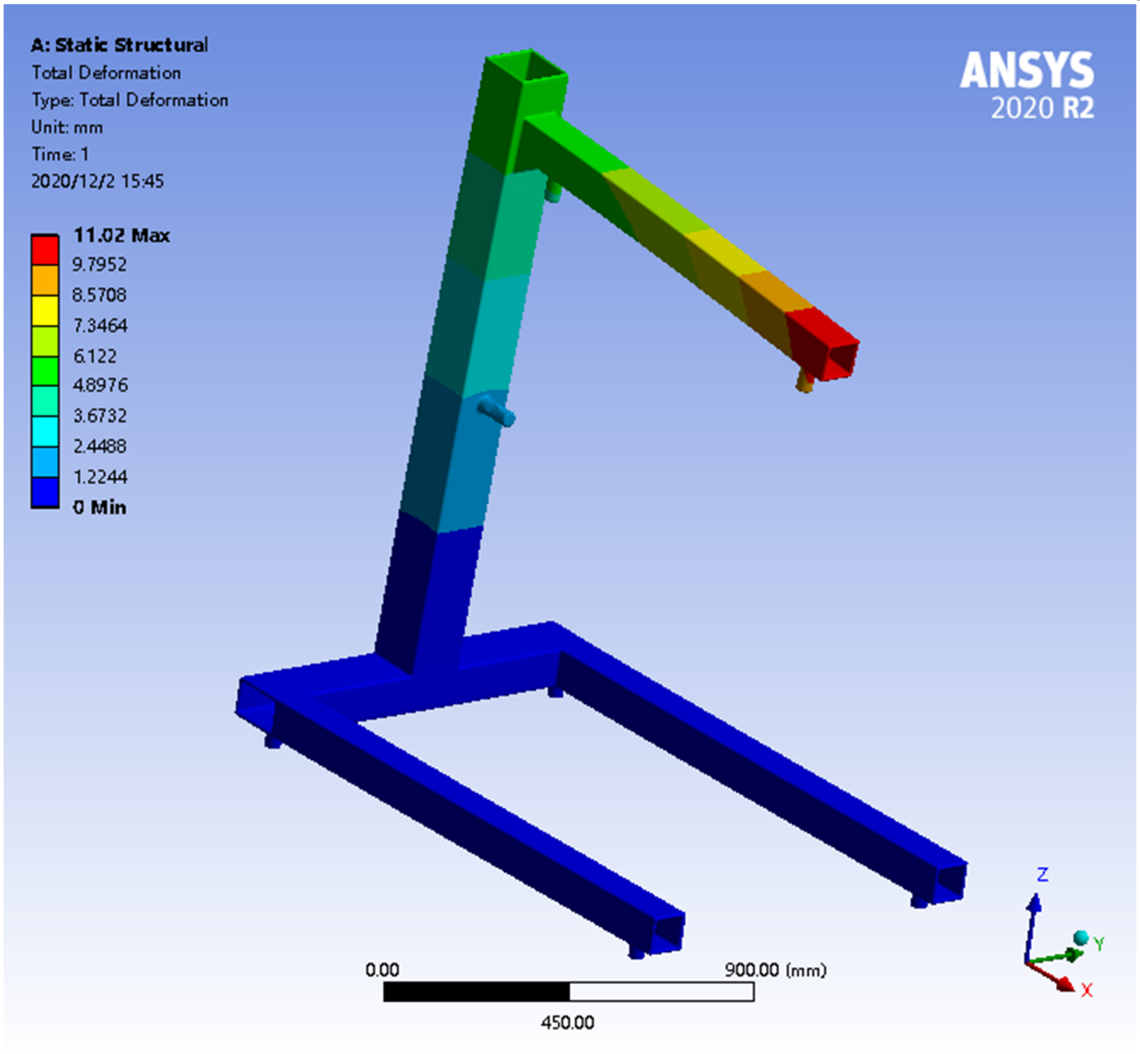

FIGURE 30 TOTAL DEFORMATION FOR THIRD DESIGN OF FLOOR CRANES

TABLE 14 TOTAL DEFORMATION FOR THIRD DESIGN OF FLOOR CRANES

Time [s]	Minimum [mm]	Maximum [mm]	Average [mm]
1.	0.	11.02	5.4222

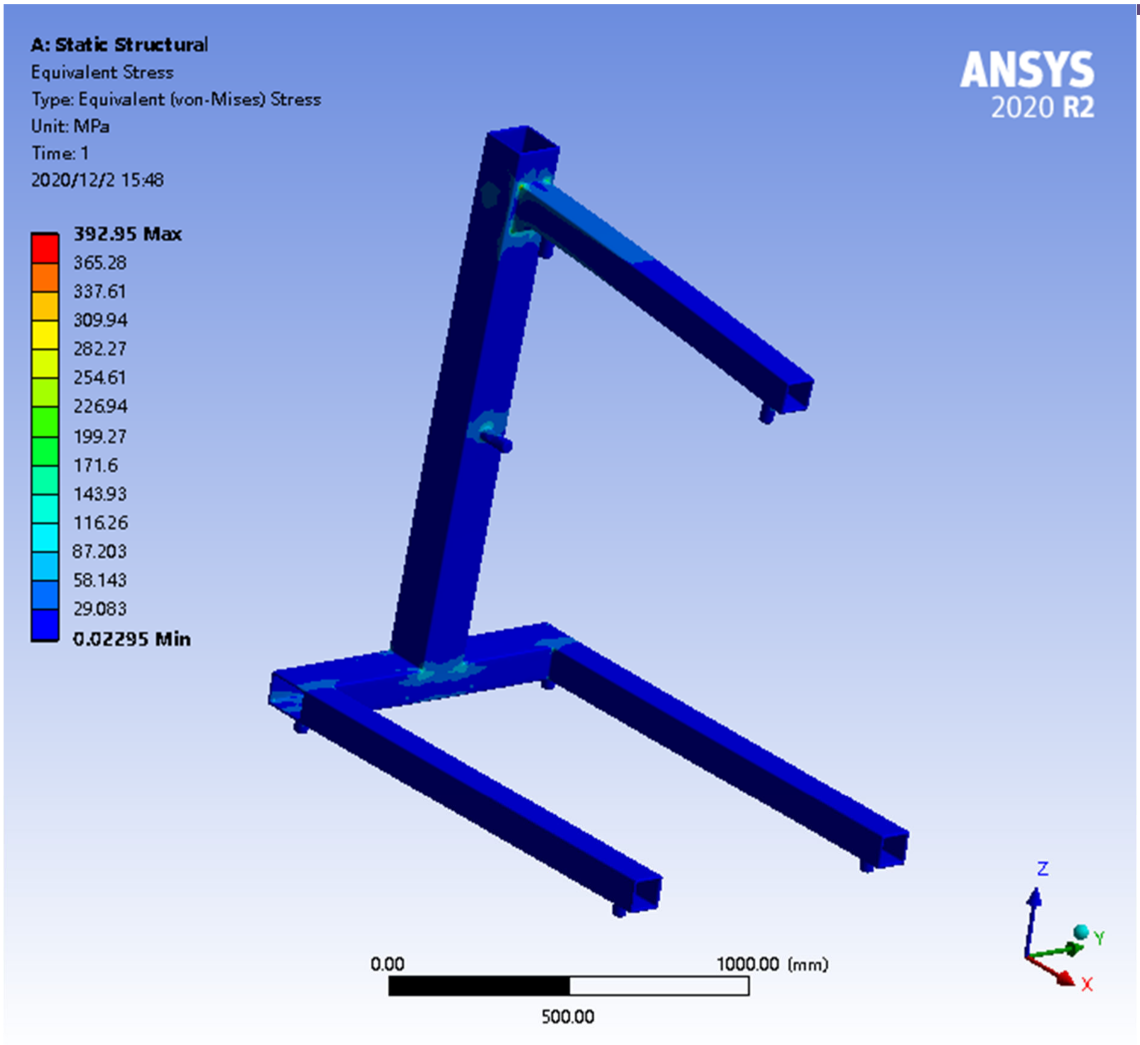

FIGURE 31 EQUIVALENT STRESS FOR THIRD DESIGN OF FLOOR CRANES

TABLE 15 EQUIVALENT STRESS FOR THIRD DESIGN OF FLOOR CRANES

Time [s]	Minimum [MPa]	Maximum [MPa]	Average [MPa]
1.	2.295e-002	392.95	22.425

From the analysis results shown in figures and tables above, I can know that the stress concentration still exists near the upper section of the intersection between the vertical column and the horizontal arm, which has still exceeded the yielding strength of ASTM A500, Grade B steel. Therefore, the third design for the floor cranes has failed.

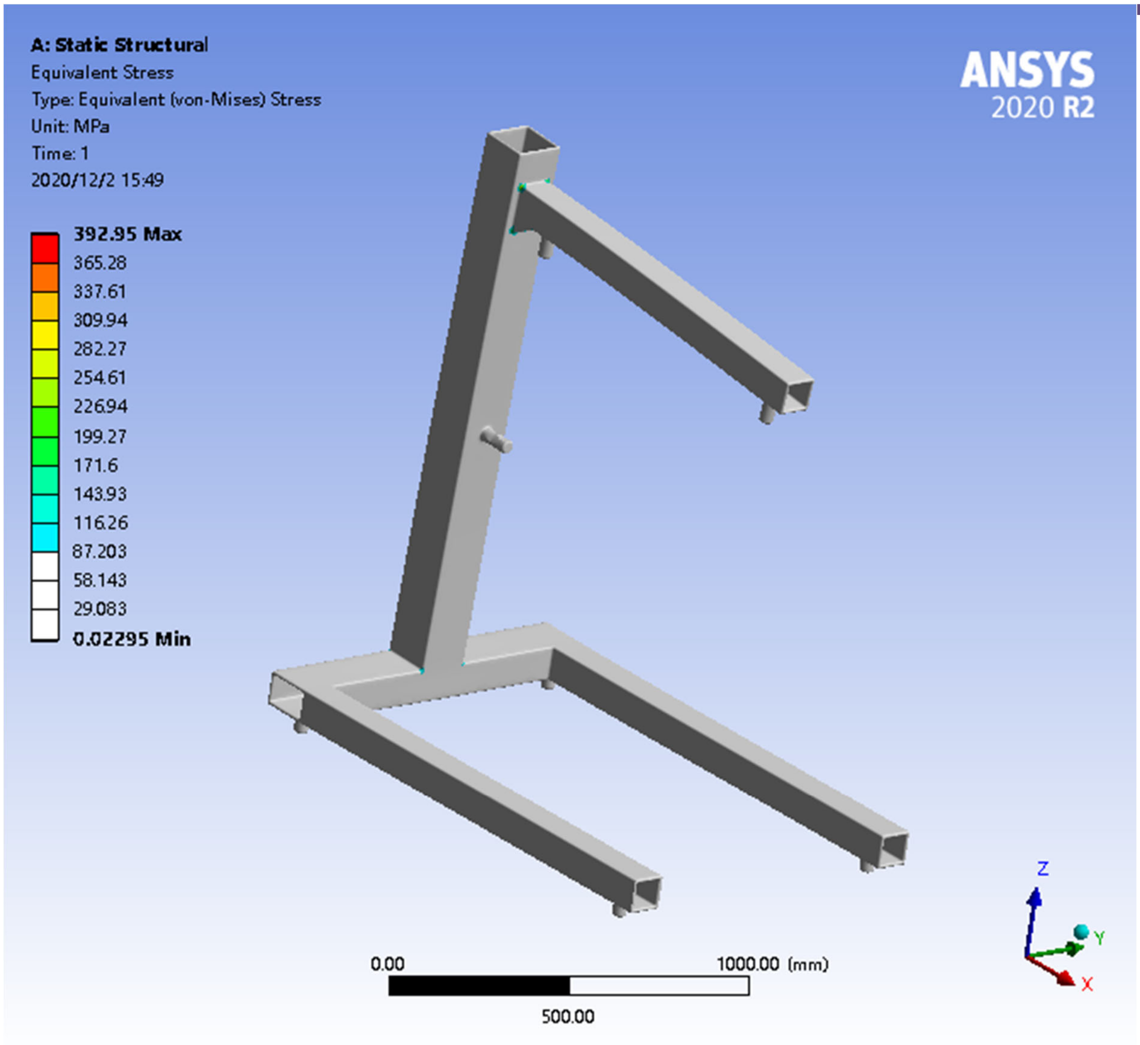

FIGURE 32 CHANG OF GRADIENT COLOR

In the figure above, I change the color of stress between 0.02295 MPa and 87.203 MPa to the white. This change lets me know the location of the high stress more clearly.

From the figure above, I can see that the stress of the most of area of the floor cranes is lower than 87.203 MPa. Only a small region has relatively high stress.

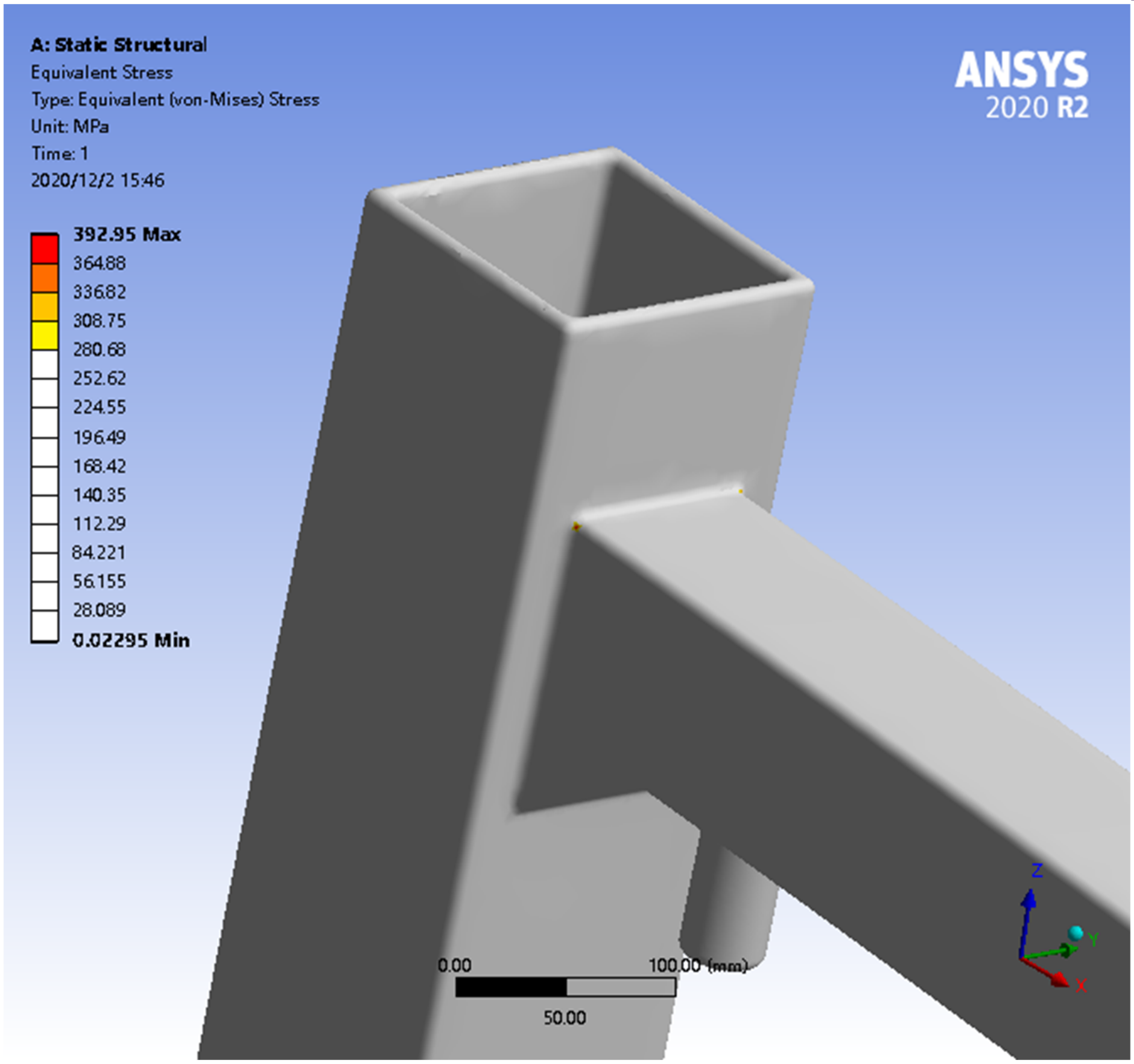

FIGURE 33 ZOOM IN OF EQUIVALENT STRESS FOR THIRD DESIGN OF FLOOR CRANES

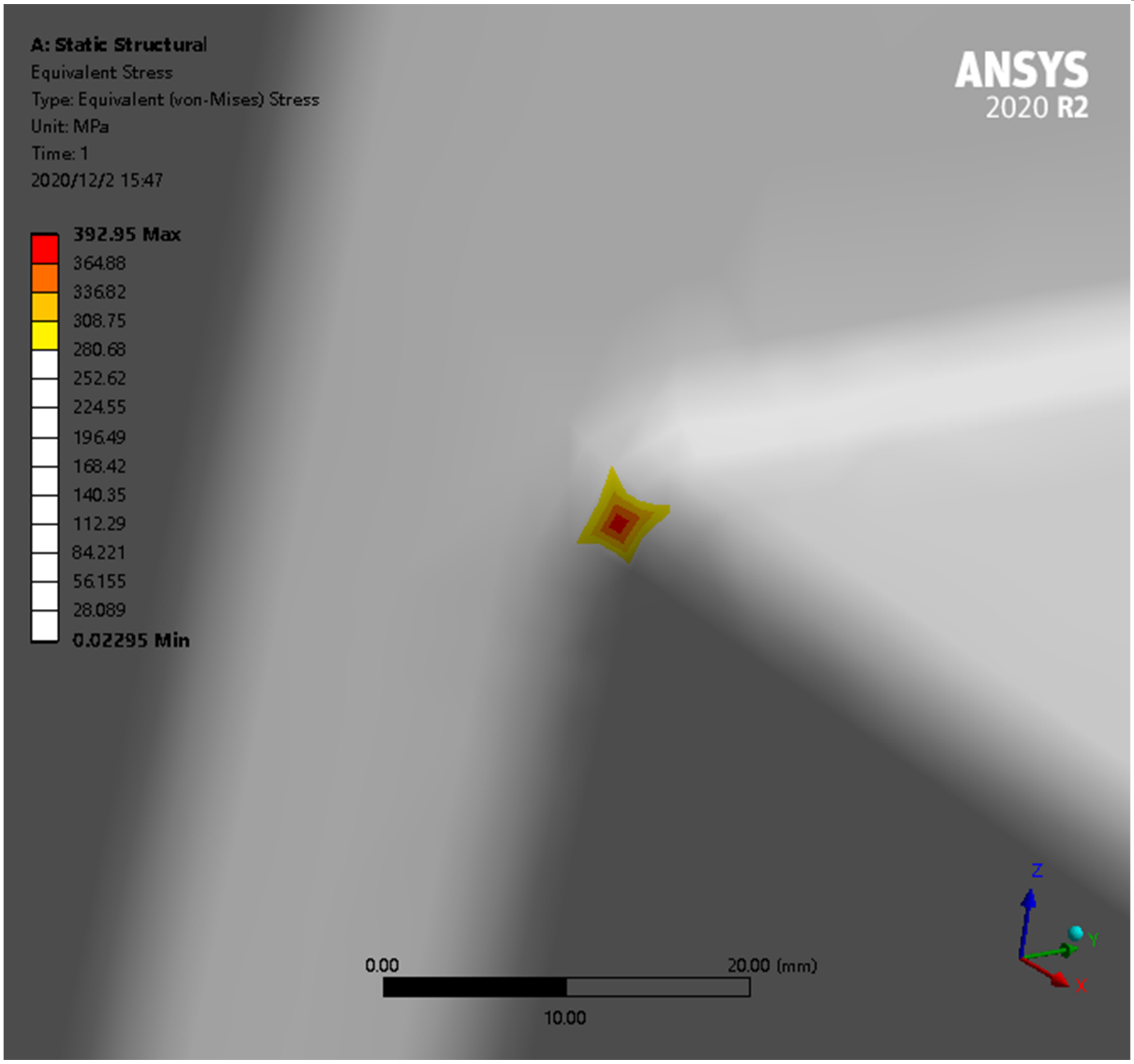

FIGURE 34 ZOOM IN OF EQUIVALENT STRESS FOR THIRD DESIGN OF FLOOR CRANES

From the figures above, I can know that the high stress only exists in a very small region, which is almost a point. Therefore, in order to improve this design. I need to reduce the stress concentration just near that point.

Due to the large stress concentration of the floor crane in the second design, I begin my fourth design to solve this problem.

3.5 Fourth (Final) Design for Floor Cranes

The problem in my third design is that the stress concentration near the upper section of the intersection between the vertical column and the horizontal arm is too large. Therefore, in this design, I try to reduce the stress concentration near this location. In order to do this, one of the ideas is to add another triangular prism between the vertical column and the horizontal arm, which is shown in figure below.

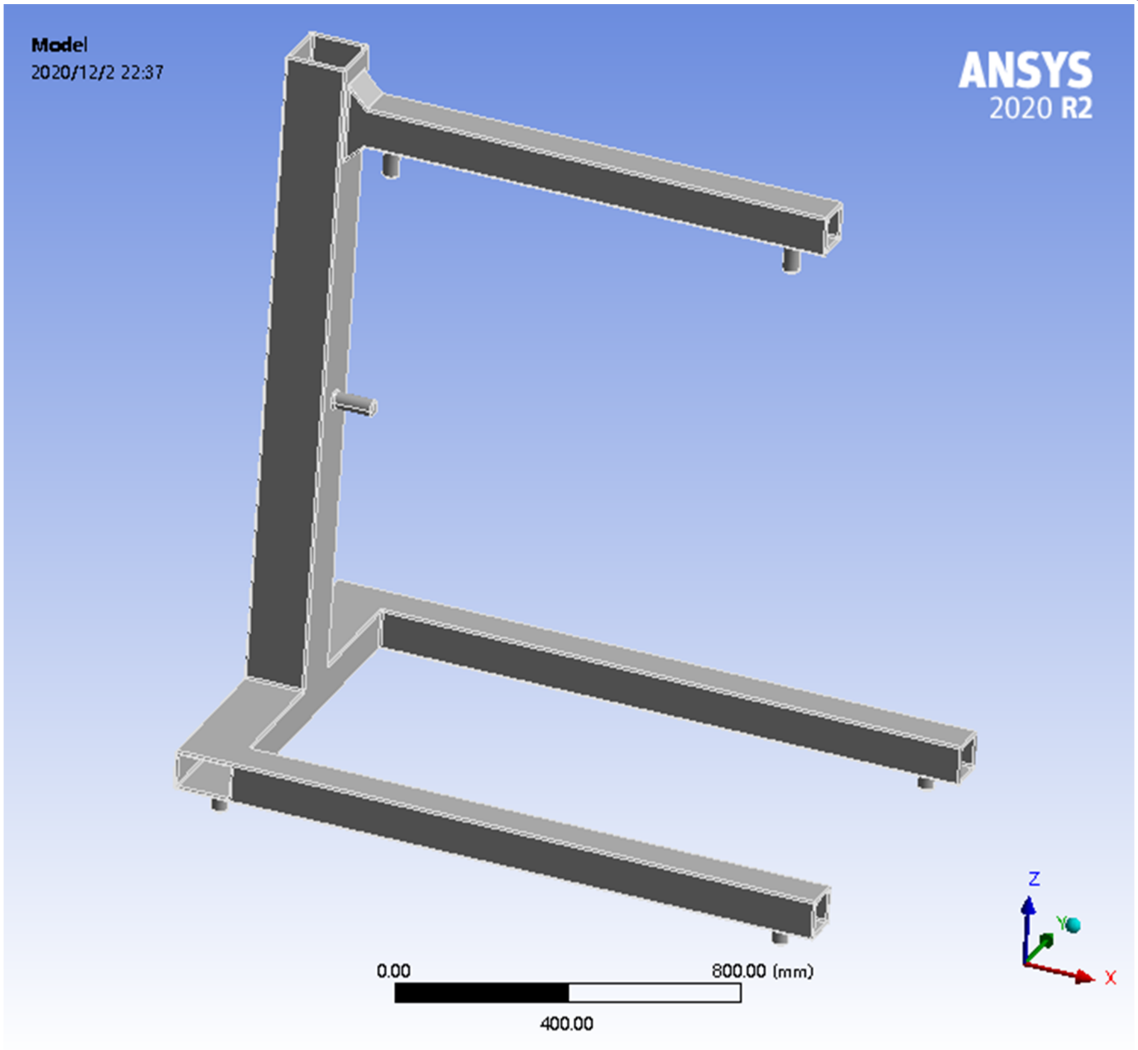

FIGURE 35 FOURTH DESIGN OF FLOOR CRANES

From the tables below, I can find that the mass of the whole part is still low relatively.

TABLE 16 BOUNDING BOX OF FOURTH DESIGN OF FLOOR CRANES

Bounding Box	
Length X	1600. mm
Length Y	1000. mm
Length Z	1750. mm

TABLE 17 PROPERTIES OF FOURTH DESIGN OF FLOOR CRANES

Properties	
Volume	2.9131e+007 mm³
Mass	228.68 kg
Centroid X	473.28 mm
Centroid Y	-0.13384 mm
Centroid Z	558.82 mm

Moment of Inertia Ip1	1.1413e+008 kg·mm²
Moment of Inertia Ip2	1.4445e+008 kg·mm²
Moment of Inertia Ip3	7.1031e+007 kg·mm²

The 3D Sketch and the dimensions of the second design are shown in figure below.

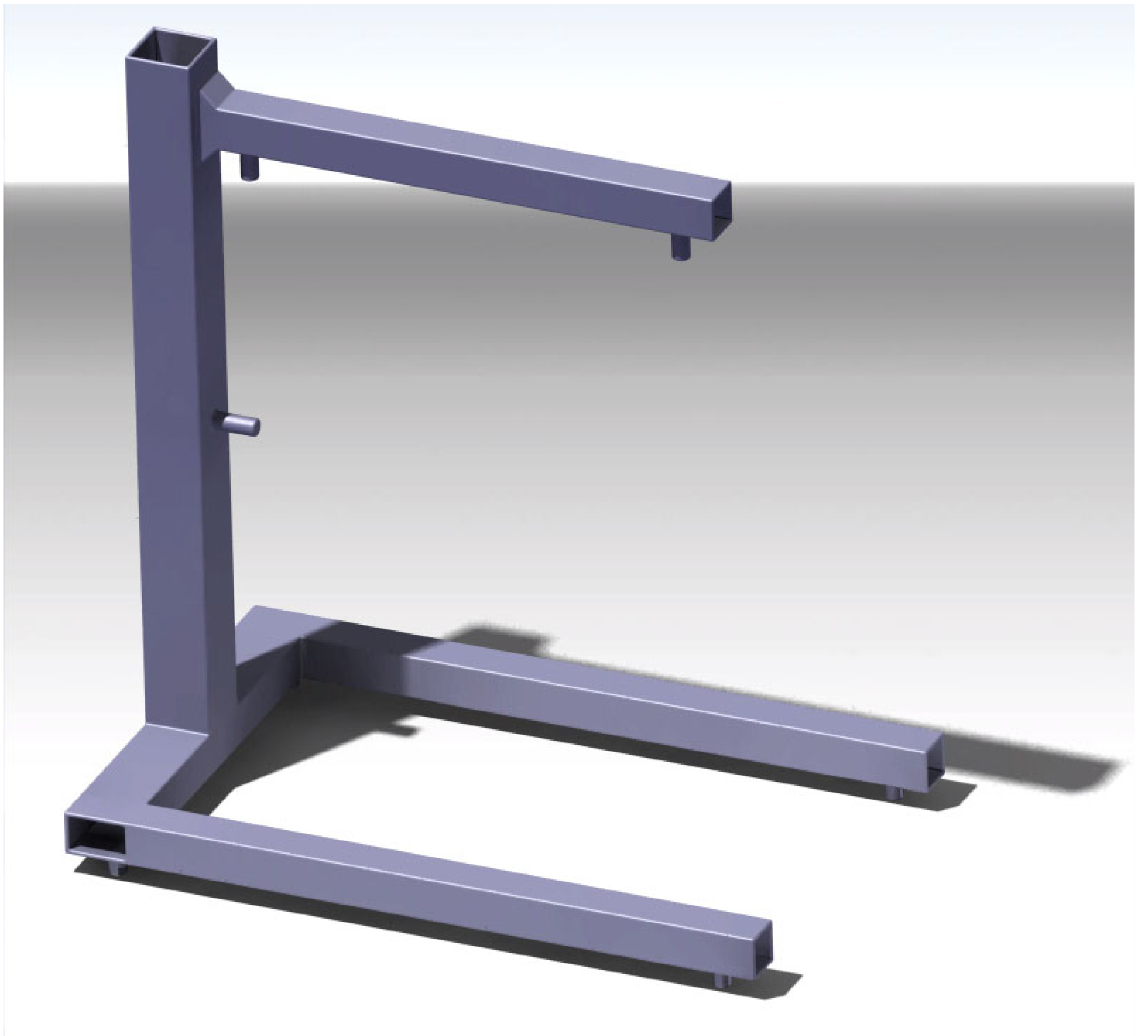

FIGURE 36 SKETCH FOR FOURTH DESIGN OF FLOOR CRANES

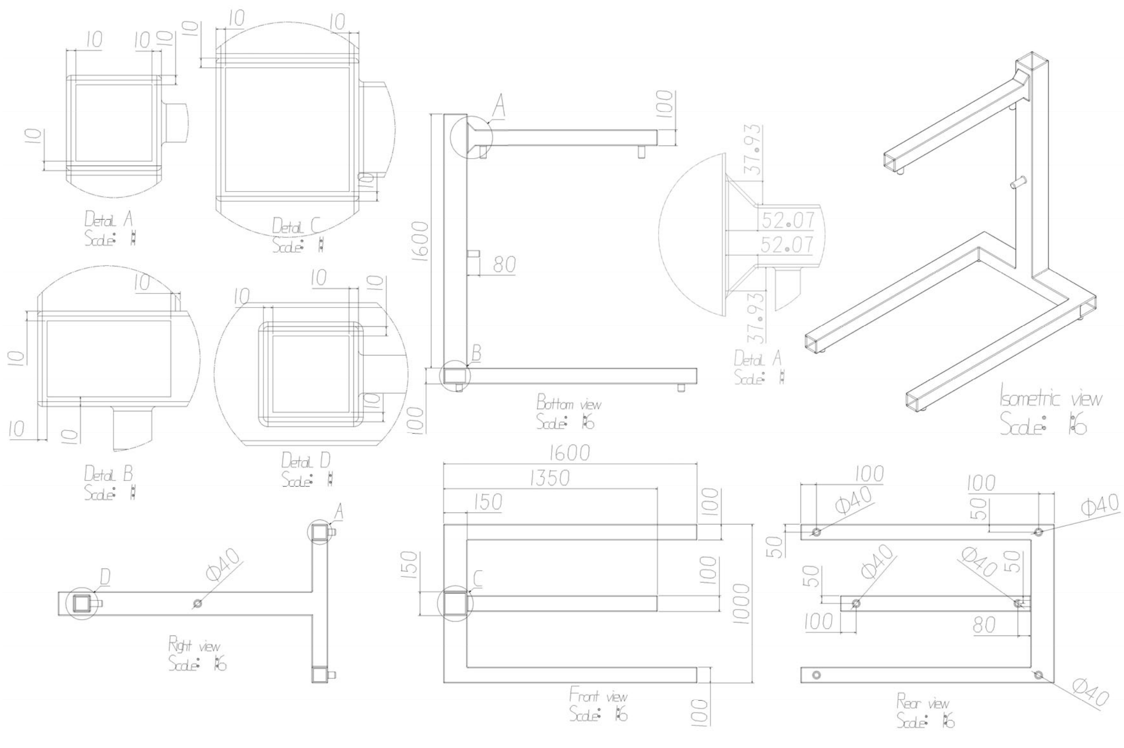

FIGURE 37 DIMENSIONS FOR FOURTH DESIGN OF FLOOR CRANES

Next, let me check the mechanics behavior of the third design to determine whether the structure meets the need to support the 400 kg weight. Here are the figures for analysis from ANSYS.

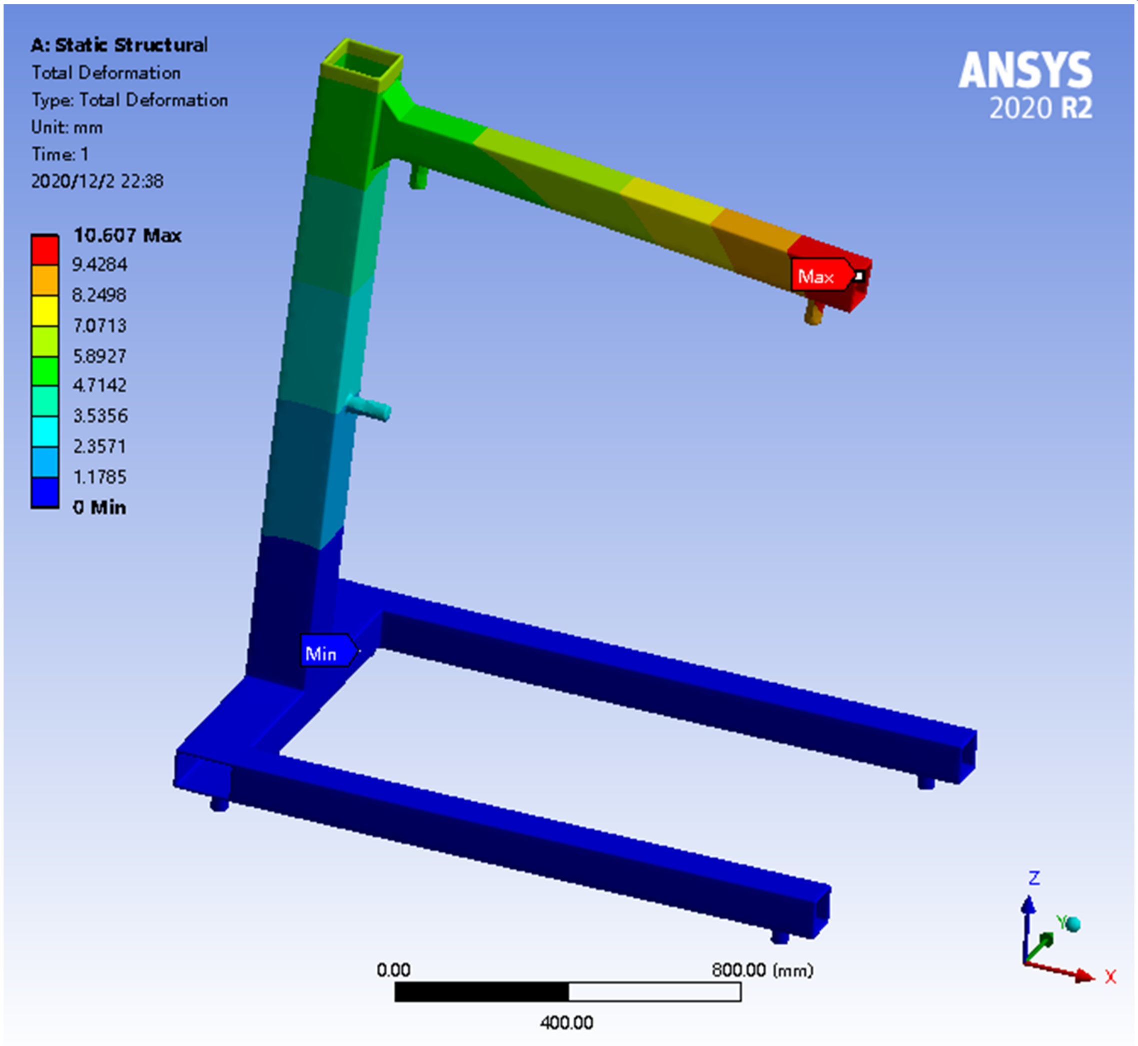

FIGURE 38 TOTAL DEFORMATION FOR FOURTH DESIGN OF FLOOR CRANES

TABLE 18 TOTAL DEFORMATION FOR FOURTH DESIGN OF FLOOR CRANES

Time [s]	Minimum [mm]	Maximum [mm]	Average [mm]
1.	0.	10.607	4.6573

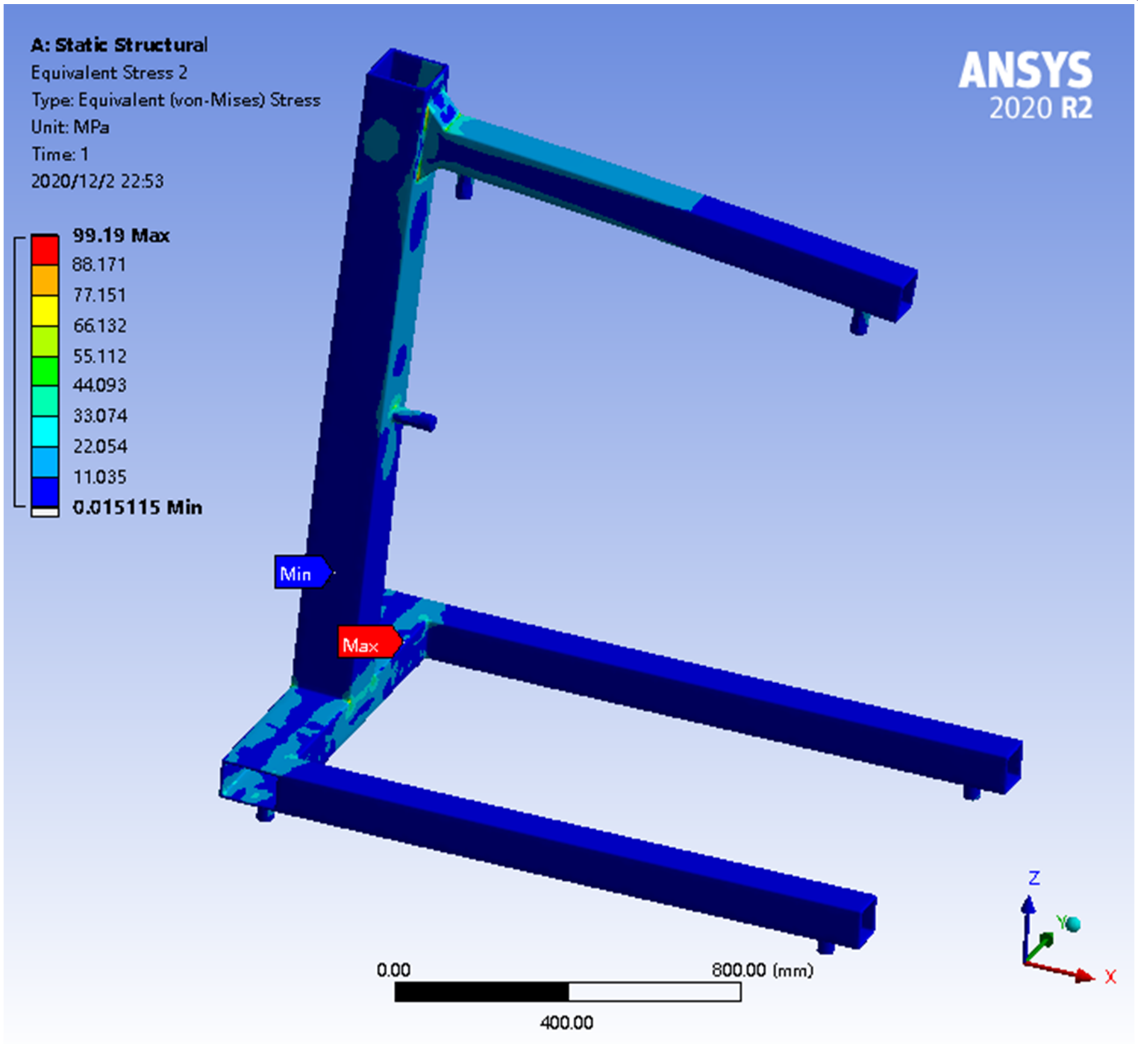

FIGURE 39 EQUIVALENT STRESS FOR FOURTH DESIGN OF FLOOR CRANES

TABLE 19 EQUIVALENT STRESS FOR FOURTH DESIGN OF FLOOR CRANES

Time [s]	Minimum [MPa]	Maximum [MPa]	Average [MPa]
1.	1.5115e-002	99.19	40.358

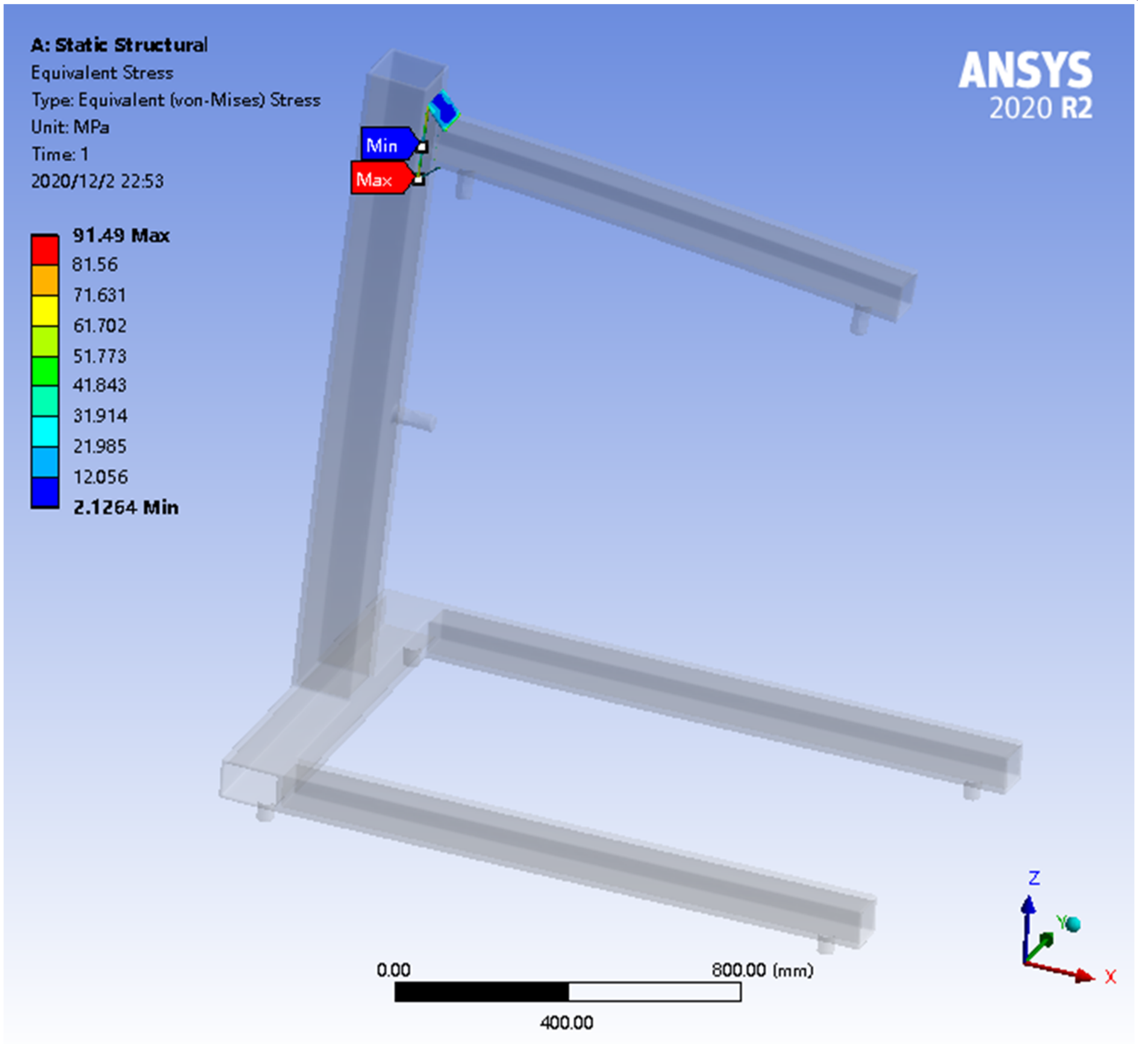

FIGURE 40 EQUIVALENT STRESS IN THE HIGH STRESS REGION

TABLE 20 EQUIVALENT STRESS IN THE HIGH STRESS REGION

Time [s]	Minimum [MPa]	Maximum [MPa]	Average [MPa]
1.	2.1264	91.49	43.448

From the analysis results shown in figures and tables above, I can know that in this design, the problems of large mass and the large stress concentration near the intersection between the vertical column and horizontal arm has solved. According to the data in the ANSYS, the maximum equivalent stress in this design is equal to 91.49 MPa, so the mechanics behavior of it is pretty good. Therefore, the factor of safety for this design can be $FS = \frac{315\ \text{MPa}}{91.49\ \text{MPa}} = 3.4$, which is very safe.

And also, I check the maximum total deflection of my fourth design, which is equal to 10.607 mm. Compared to the total length of the horizontal arm, which is equal to 1200 mm, this maximum total deflection is quite small.

4 Analysis for Design of Floor Cranes

4.1 Floor Load Analysis

Floor load is a measure of pressure on the floor of truck. It is necessary to avoid the catastrophic failure.

TABLE 21 BOUNDING BOX OF FOURTH DESIGN OF FLOOR CRANES

Bounding Box	
Length X	1600. mm
Length Y	1000. mm
Length Z	1750. mm

TABLE 22 PROPERTIES OF FOURTH DESIGN OF FLOOR CRANES

Properties	
Volume	2.9131e+007 mm³
Mass	228.68 kg
Centroid X	473.28 mm
Centroid Y	-0.13384 mm
Centroid Z	558.82 mm
Moment of Inertia Ip1	1.1413e+008 kg·mm²
Moment of Inertia Ip2	1.4445e+008 kg·mm²
Moment of Inertia Ip3	7.1031e+007 kg·mm²

From the tables above, I can get the total weight of the equipment after loading the $400\ \text{kg}$ mass is equal to $400\ \text{kg} + 228.68\ \text{kg} = 628.68\ \text{kg}$. In addition, the length and the breadth of the floor crane are equal to $1600\ \text{mm}$ and $1000\ \text{mm}$, respectively. Therefore, the floor load of the whole device is equal to

$$P = \frac{F}{A} = \frac{[(400\ \text{kg}) + (228.68\ \text{kg})] \times (9.81\ \text{m/s}^2)}{(1600\ \text{mm}) \times (1000\ \text{mm})} = 3855\ \text{Pa}$$

4.2 Main Body Analysis

The free-body diagram of the main body is shown in figure below.

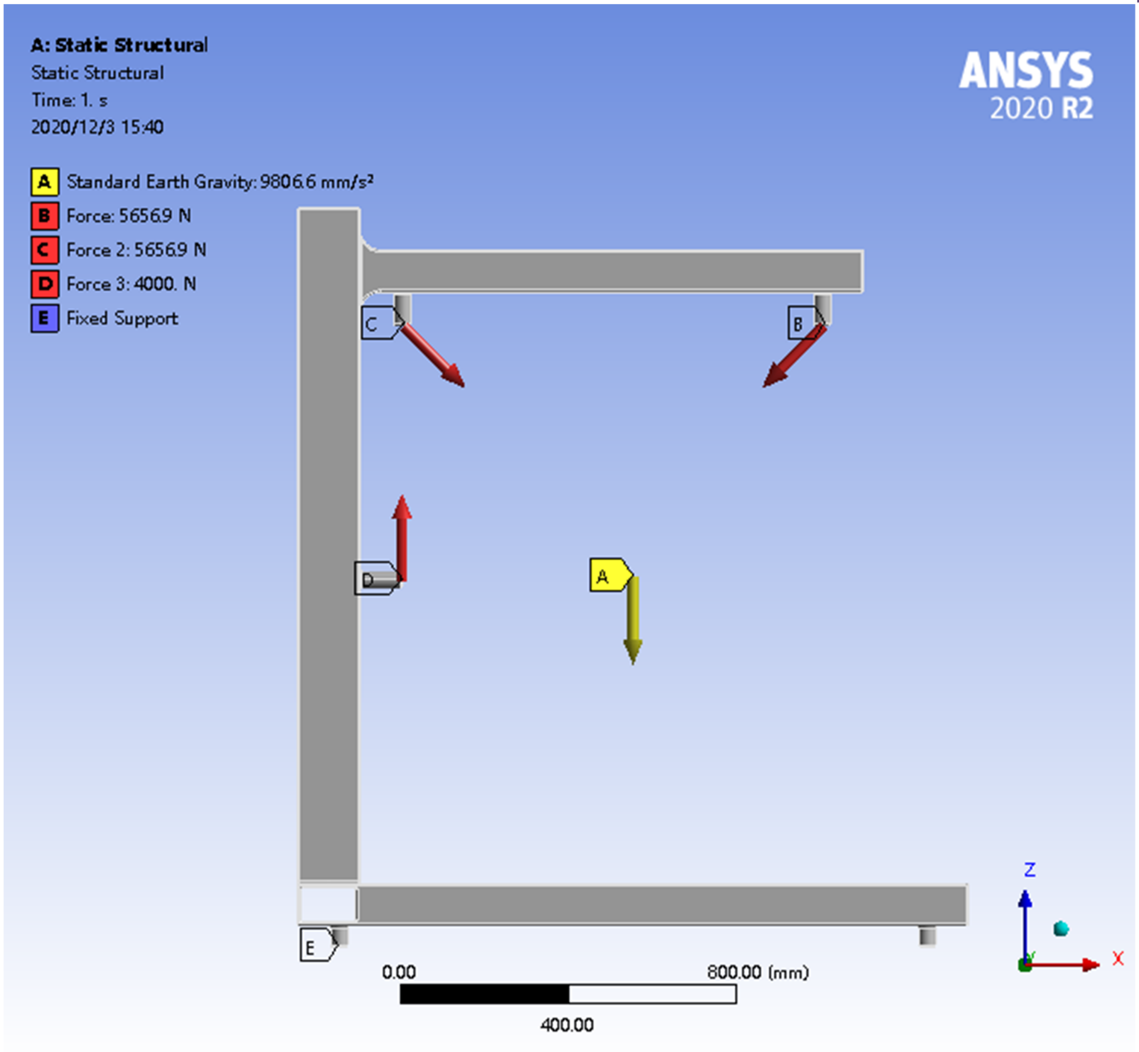

FIGURE 41 FREE-BODY DIAGRAM OF THE MAIN BODY

In order to simplify the analysis, I divided my analysis for the main body into three parts—horizontal arm, vertical column, and the base.

4.2.1 HORIZONTAL ARM ANALYSIS

The free-body diagram of the horizontal arm is shown in figure below:

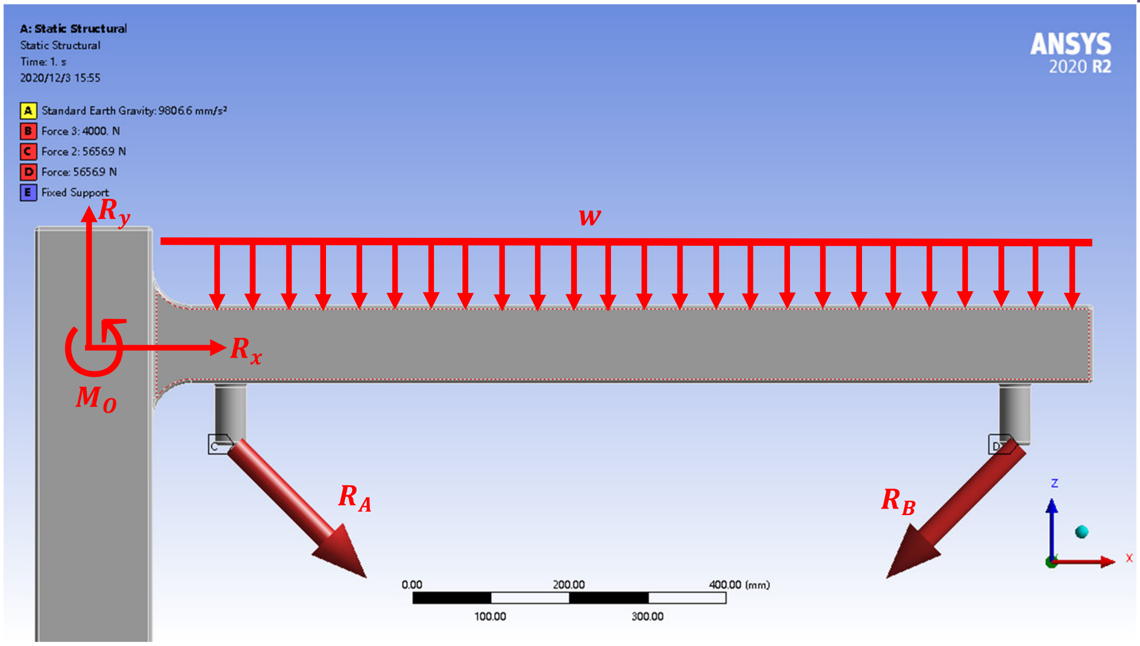

FIGURE 42 FREE-BODY DIAGRAM OF THE HORIZONTAL ARM

4.2.1.1 MAXIMUM STRESS ANALYSYS

From the free-body diagram of the horizontal arm, I can get the equation shown below:

$$\sum F_x = 0 \Longrightarrow R_x + R_A \cos 45° - R_B \cos 45° = 0$$

$$\sum F_y = 0 \Longrightarrow R_y - R_A \sin 45° - R_B \sin 45° - wL = 0$$

$$\sum M_O = 0 \Longrightarrow M_O - R_A \cos 45° \, x_1 - R_B \cos 45° \, x_2 - \int_0^L wx dx = 0$$

in which

$$\begin{cases} R_x \cos 45° = 4000 \text{ N} \\ R_A \sin 45° = 4000 \text{ N} \\ R_B \cos 45° = 4000 \text{ N} \\ R_B \sin 45° = 4000 \text{ N} \\ w = \rho g A = (7.89 \times 10^3 \text{ kg/m}^3) \times (9.806 \text{ m/s}^2) \times [(0.1 \text{ m})^2 - (0.08 \text{ m})^2] = 278.5 \text{ N/m} \\ L = 1.2 \text{ m} \\ x_1 = 0.08 \text{ m} \\ x_2 = 1.1 \text{ m} \end{cases}$$

Therefore, from the information above, I can solve the equation and get that

$$\begin{cases} R_x = 0 \\ R_y = 8334.24 \text{ N} \\ M = 4920.52 \text{ N} \cdot \text{m} \end{cases}$$

Then I can know that the shearing force and the bending moment along the beam are equal to

$$V(x) = \begin{cases} 8334.24 - 278.5x, 0 \leq \mathrm{x} < 0.08\ \mathrm{m} \\ 4334.24 - 278.5x, 0.08 \leq \mathrm{x} < 1.1\ \mathrm{m} \\ 334.24 - 278.5x, 1.1 \leq \mathrm{x} < 1.2\ \mathrm{m} \end{cases}$$

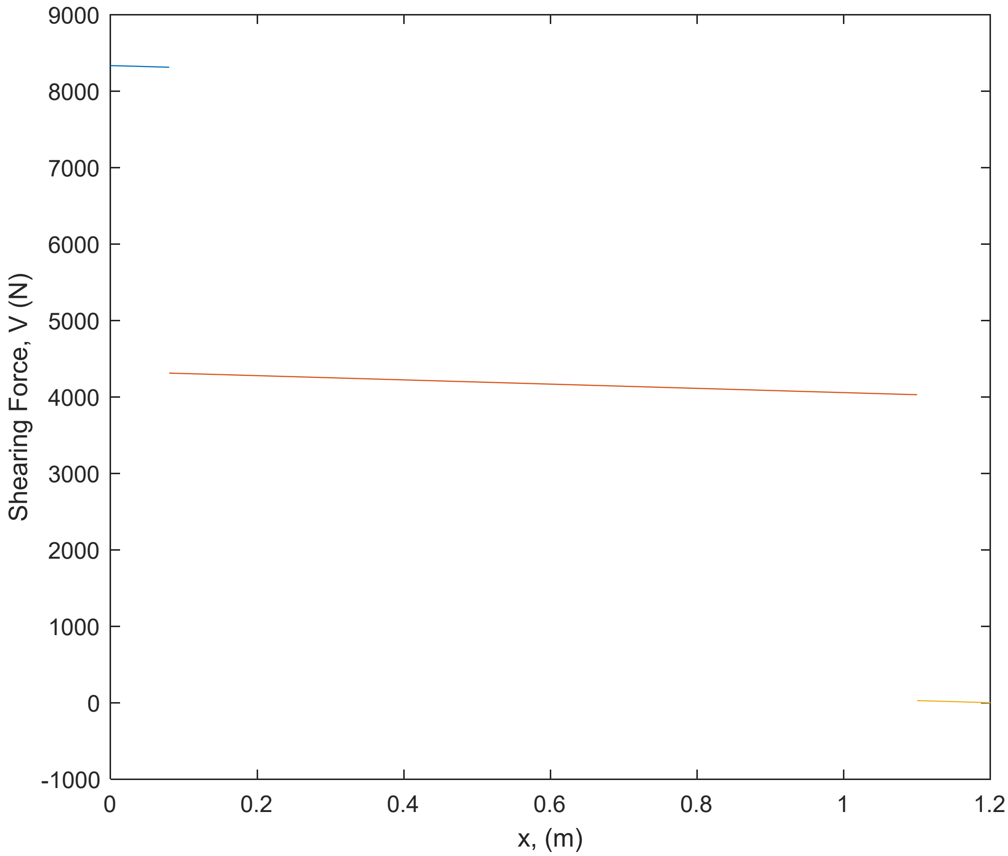

FIGURE 43 SHEARING STRESS ALONG THE HORIZONTAL ARM

$$M(x) = \begin{cases} 8334.24x - \dfrac{278.5}{2}x^2 - 4920.52, 0 \leq \mathrm{x} < 0.08\ \mathrm{m} \\ 4334.24x - \dfrac{278.5}{2}x^2 - 4590.27, 0.08 \leq \mathrm{x} < 1.1\ \mathrm{m} \\ 334.24x - \dfrac{278.5}{2}x^2 - 190.27, 1.1 \leq \mathrm{x} < 1.2\ \mathrm{m} \end{cases}$$

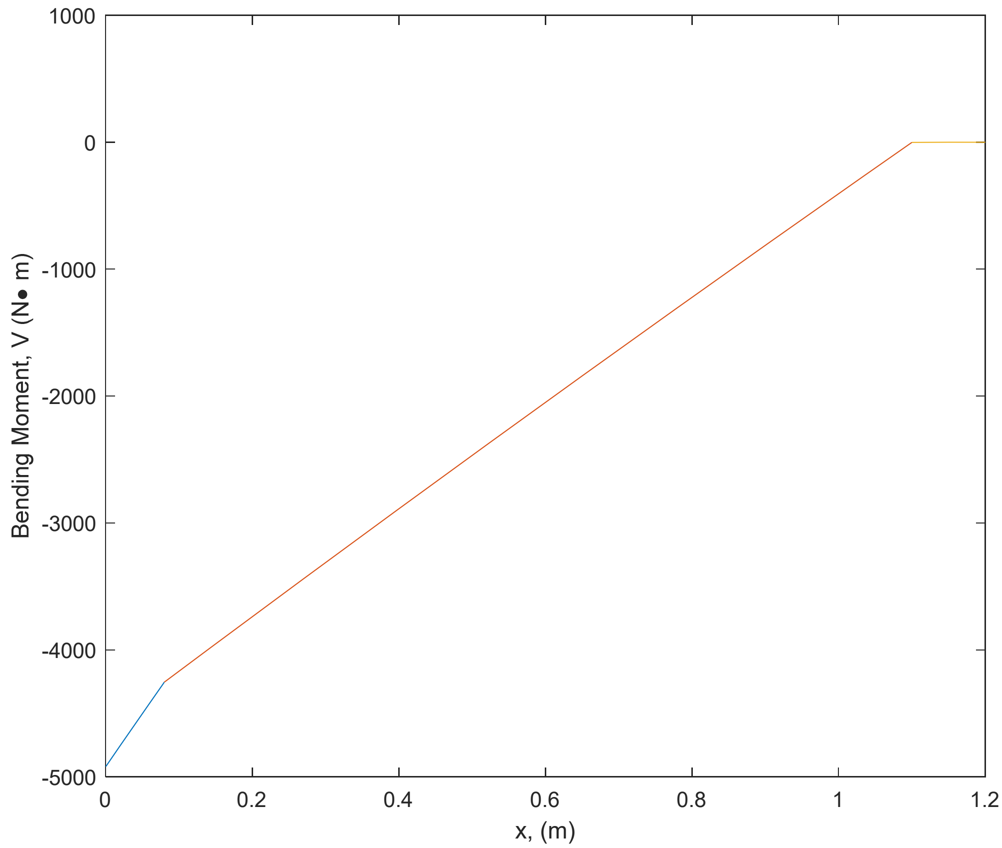

FIGURE 44 BENDING MOMENT ALONG THE HORIZONTAL ARM

Adding the second moments of area for the two parts gives the second moment of area for the cross section as

$$I = \frac{(0.1\text{ m}) \times (0.1\text{ m})^3}{12} - \frac{(0.08\text{ m}) \times (0.08\text{ m})^3}{12} = 4.92 \times 10^{-6}\text{ m}^4$$

From the bending moment diagram, I can know that the maximum bending moment occurs near the intersection between the horizontal arm and the vertical column. Since the resisting moment M is negative, the top portion of the beam is in tension (σ positive) and the bottom portion of the beam is in compression (σ negative). The flexural stress varies linearly with distance from the neutral axis. Therefore, the maximum tensile flexural stress occurs at the top surface of the beam

$$\sigma_{max} = -\frac{My}{I} = -\frac{(4920.52\text{ N}\cdot\text{m}) \times (0.05\text{ m})}{(4.92 \times 10^{-6}\text{ m}^4)} = 50.00\text{ MPa}$$

Also from the free-body diagram of the horizontal arm, I can learn that the region between two pulleys has the compression due to the horizontal component of the force on the pulleys, which are $R_A \sin 45°$ and $R_B \sin 45°$. Therefore, we cannot only consider the tensile flexural stress. Instead, we need to add the compression mentioned. Therefore, I plot the stresses on the top and bottom of the horizontal arm.

First, let me express the stresses on the top and the bottom of horizontal arm as show below:

$$\sigma_{topmax} = -\frac{M(x)y}{I} = M(x)$$

$$= \begin{cases} -\dfrac{\left(8334.24x - \dfrac{278.5}{2}x^2 - 4920.52\right) \times (0.05\ \mathrm{m})}{(4.92 \times 10^{-6}\ \mathrm{m}^4)}, 0 \leq \mathrm{x} < 0.08\ \mathrm{m} \\ -\dfrac{\left(4334.24x - \dfrac{278.5}{2}x^2 - 4590.27\right) \times (0.05\ \mathrm{m})}{(4.92 \times 10^{-6}\ \mathrm{m}^4)} - \dfrac{(4000\ \mathrm{N})}{[(0.1\ \mathrm{m})^2 - (0.08\ \mathrm{m})^2]}, 0.08 \leq \mathrm{x} < 1.1\ \mathrm{m} \\ -\dfrac{\left(334.24x - \dfrac{278.5}{2}x^2 - 190.27\right) \times (0.05\ \mathrm{m})}{(4.92 \times 10^{-6}\ \mathrm{m}^4)}, 1.1 \leq \mathrm{x} < 1.2\ \mathrm{m} \end{cases}$$

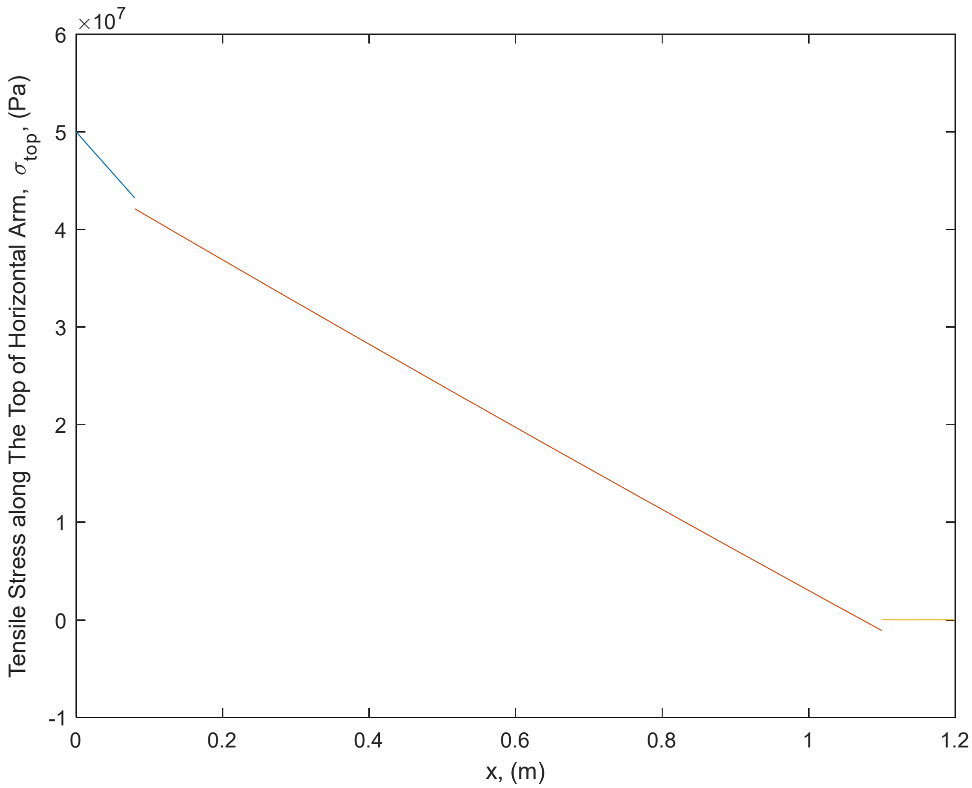

FIGURE 45 TENSILE STRESS ALONG THE TOP OF HORIZONTAL ARM

$$\sigma_{bottommax} = -\frac{M(x)y}{I} = M(x)$$

$$= \begin{cases} \dfrac{\left(8334.24x - \dfrac{278.5}{2}x^2 - 4920.52\right) \times (0.05\ \mathrm{m})}{(4.92 \times 10^{-6}\ \mathrm{m}^4)}, 0 \leq \mathrm{x} < 0.08\ \mathrm{m} \\ \dfrac{\left(4334.24x - \dfrac{278.5}{2}x^2 - 4590.27\right) \times (0.05\ \mathrm{m})}{(4.92 \times 10^{-6}\ \mathrm{m}^4)} - \dfrac{(4000\ \mathrm{N})}{[(0.1\ \mathrm{m})^2 - (0.08\ \mathrm{m})^2]}, 0.08 \leq \mathrm{x} < 1.1\ \mathrm{m} \\ \dfrac{\left(334.24x - \dfrac{278.5}{2}x^2 - 190.27\right) \times (0.05\ \mathrm{m})}{(4.92 \times 10^{-6}\ \mathrm{m}^4)}, 1.1 \leq \mathrm{x} < 1.2\ \mathrm{m} \end{cases}$$

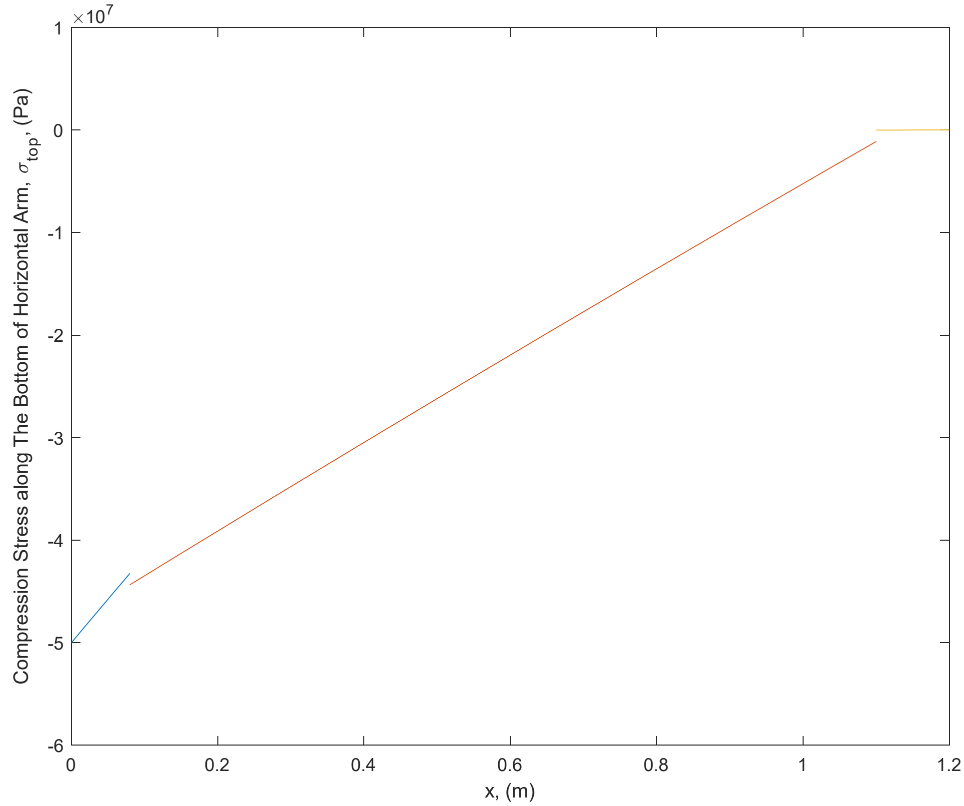

FIGURE 46 COMPRESSION STRESS ALONG THE BOTTOM OF HORIZONTAL ARM

Therefore, from the analysis above, I can know that although there is compression on the region between two pulleys, the compression is not significant. The maximum tensile flexural stress occurs at the top surface of the beam near the intersection between the horizontal arm and the vertical column, which is equal to $\sigma_{max} = 50.00$ MPa.

4.2.1.2 DEFLECTION ANALYSYS

In this design, I can divide the free-body diagram into three parts in order to use super-position method.

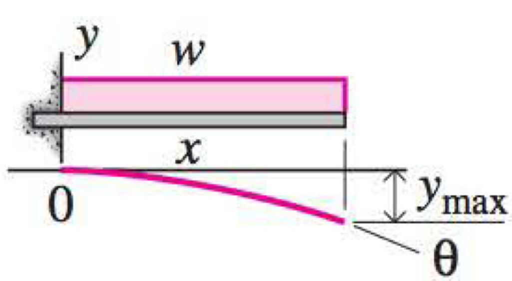

FIGURE 47 FIRST PART

The first part of the super-position is caused by the weight of the beam. I calculate the max deflection at the end of the horizontal arm.

$$y_{max} = -\frac{wL^4}{8EI} = -\frac{(278.5\ \mathrm{N/m}) \times (1.2\ \mathrm{m})^4}{8 \times (210\ \mathrm{GPa}) \times (4.92 \times 10^{-6}\ \mathrm{m}^4)} = -6.9875 \times 10^{-5}\ \mathrm{m}$$

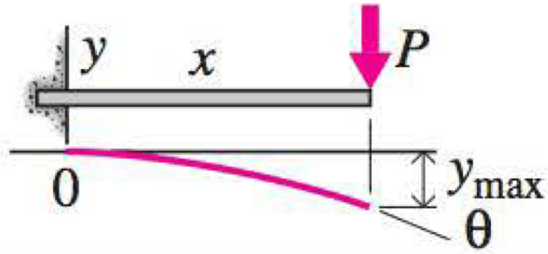

FIGURE 48 SECOND PART

The second part of the super-position is caused by the force acting along the pulleys. I calculate the max deflection at the end of the horizontal arm.

$$y_{max} = -\frac{PL^3}{3EI} = -\frac{(4000\ \mathrm{N}) \times (0.08\ \mathrm{m})^3}{3 \times (210\ \mathrm{GPa}) \times (4.92 \times 10^{-6}\ \mathrm{m}^4)}$$

$$+ [(1.2\ \mathrm{m}) - (0.08\ \mathrm{m})] \times \sin\left[-\frac{(4000\ \mathrm{N}) \times (0.08\ \mathrm{m})^2}{2 \times (210\ \mathrm{GPa}) \times (4.92 \times 10^{-6}\ \mathrm{m}^4)}\right]$$

$$= -1.4536 \times 10^{-5}\ \mathrm{m}$$

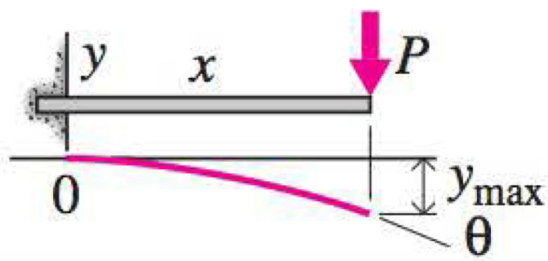

FIGURE 49 THIRD PART

The second part of the super-position is caused by the force acting along the pulleys. I calculate the max deflection at the end of the horizontal arm.

$$y_{max} = -\frac{PL^3}{3EI} = -\frac{(4000\ \mathrm{N}) \times (1.1\ \mathrm{m})^3}{3 \times (210\ \mathrm{GPa}) \times (4.92 \times 10^{-6}\ \mathrm{m}^4)}$$

$$+ [(1.2\ \mathrm{m}) - (1.1\ \mathrm{m})] \times \sin\left[-\frac{(4000\ \mathrm{N}) \times (1.1\ \mathrm{m})^2}{2 \times (210\ \mathrm{GPa}) \times (4.92 \times 10^{-6}\ \mathrm{m}^4)}\right]$$

$$= -0.0020\ \mathrm{m}$$

Therefore, the total deflection of the horizontal arm is almost equal to -0.0020 m, which is quite small.

4.2.2 VERTICAL COLUMN ANALYSIS

The free-body diagram of the vertical column is shown in figure below:

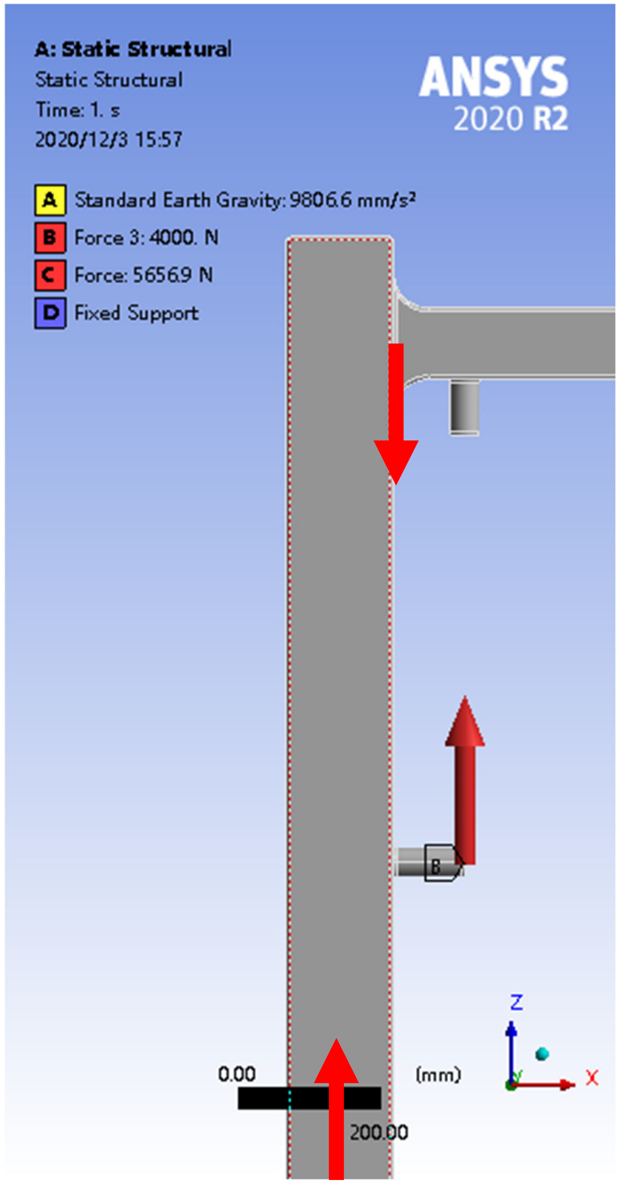

FIGURE 50 FREE-BODY DIAGRAM OF THE VERTICAL COLUMN

4.2.2.1 BUCKLING ANALYSYS

Since the column is made of steel, Code 1 of Column Codes for Centric Loading will be used to calculate σ_{all}. The equation for determining σ_{all} depends on the slenderness range.

$$C_c = \sqrt{\frac{2\pi^2 E}{\sigma_y}} = \sqrt{\frac{2\pi^2 \times (210\text{ GPa})}{(315\text{ MPa})}} = 114.7147$$

$$\frac{L}{r_{min}} = \frac{1.6\text{ m}}{0.075\text{ m}} = 21.333 < C_c = 114.7147$$

Since $\frac{L}{r_{min}} < C_c$, the intermediate column formula is applicable. The factor of safety FS for use in the intermediate column formula is

$$FS = \frac{5}{3} + \frac{3}{8}\left(\frac{L/r}{C_c}\right) - \frac{1}{8}\left(\frac{L/r}{C_c}\right)^3 = \frac{5}{3} + \frac{3}{8}\left(\frac{21.333}{114.7147}\right) - \frac{1}{8}\left(\frac{21.333}{114.7147}\right)^3 = 1.7356$$

$$\sigma_{all} = \frac{\sigma_y}{FS}\left[1 - \frac{1}{2}\left(\frac{L/r}{C_c}\right)^2\right] = \frac{(315\ \text{MPa})}{(1.7186)}\left[1 - \frac{1}{2}\left(\frac{21.333}{114.7147}\right)^2\right] = 178.3549\ \text{MPa} = \sigma_\text{a}$$

4.2.2.1.1 Allowable Stress Method

Using the allowable stress method gives

$$\frac{P}{A} + \frac{Mc}{I} = \frac{P}{A} + \frac{Prc}{I} \le \sigma_{all}$$

$$\frac{P}{[(0.15\ \text{m})^2 - (0.13\ \text{m})^2]} + \frac{P(0.075\ \text{m})(0.075\ \text{m})}{\frac{(0.15\ \text{m})(0.15\ \text{m})^3}{12} - \frac{(0.13\ \text{m})(0.13\ \text{m})^3}{12}} \le 178.3549\ \text{MPa}$$

$$P \le 3.6812 \times 10^5\ \text{N}$$

Therefore, the maximum safe load that can be applied according to the allowable stress method is

$$P_{max} = 3.6812 \times 10^5\ \text{N}$$

And according to analysis above, I can know that the loading on the edge of the vertical column is equal to 8334.24 N. Therefore, the column is pretty safe.

4.2.2.1.2 Allowable Stress Method

Using the interaction method gives

$$\frac{P/A}{\sigma_a} + \frac{Mc/I}{\sigma_b} = \frac{P/A}{\sigma_a} + \frac{Prc/I}{\sigma_b} \le 1$$

$$\frac{P/[(0.15\ \text{m})^2 - (0.13\ \text{m})^2]}{(178.3549\ \text{MPa})} + \frac{P(0.075\ \text{m})(0.075\ \text{m})/\left[\frac{(0.15\ \text{m})(0.15\ \text{m})^3}{12} - \frac{(0.13\ \text{m})(0.13\ \text{m})^3}{12}\right]}{(190\ \text{MPa})} \le 1$$

$$P \le 3.8294 \times 10^5\ \text{N}$$

Therefore, the maximum safe load that can be applied according to the interaction method is

$$P_{max} = 3.8294 \times 10^5\ \text{N}$$

And according to analysis above, I can know that the loading on the edge of the vertical column is equal to 8334.24 N. Therefore, the column is pretty safe.

4.2.3 Base Analysis

Because the base on the floor crane is relatively large and stable, the possibility of the failure occurring at the horizontal arm and the vertical column is relatively high. Therefore, according to all the analysis above, I can know that there is no failure occurs at the base.

4.3 Hook Analysis

The hooks used in various types of cranes play a major role in lifting the heavy loads in many sectors, industries, oil rigs, vehicles, etc. The performance of the hook depends on its load rating. Even though the hook may have high load rating, the failure of the hooks has many reasons such as the bearing used in the hook block, types of fastening system by which they are fastened to the hoists or cranes, materials used in the design of the hook, etc.

The hooks used for heavy loads also need to be large, big, huge and heavy in order to function safely at the prescribed loads. Due to this various types of researchers are taking place in the field of manufacturing of hooks such as process by which they are manufactured, metallurgy involved in the manufacturing, etc., in order to reduce the size, cost of manufacturing and to increase the flexibility in the usage of the hooks which can be used for high loads.

4.3.1 Hook Stress Analysis

The free-body diagram of the hook is shown in figure below:

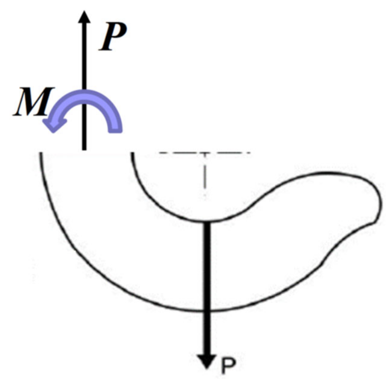

FIGURE 51 FREE-BODY DIAGRAM OF THE HOOK

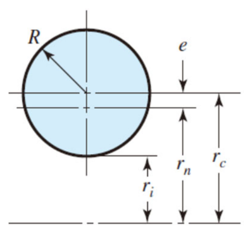

$$r_c = r_i + R$$

$$r_n = \frac{R^2}{2(r_c - \sqrt{r_c^2 - R^2})}$$

FIGURE 52 FORMULAS FOR SECTION OF CURVED BEAMS

From the figure above, I can know that

$$r_c = r_i + R$$

$$r_n = \frac{R^2}{2\left(r_c - \sqrt{r_c^2 - R^2}\right)} = \frac{R^2}{2\left[(r_i + R) - \sqrt{(r_i + R)^2 - R^2}\right]}$$

$$c_i = r_n - r_i = \frac{R^2}{2\left[(r_i + R) - \sqrt{(r_i + R)^2 - R^2}\right]} - r_i$$

Therefore, the eccentricity is equal to

$$e = (r_i + R) - \frac{R^2}{2\left[(r_i + R) - \sqrt{(r_i + R)^2 - R^2}\right]}$$

Direct tensile stress due to P is

$$\sigma_t = \frac{P}{A} = \frac{P}{\pi R^2}$$

Critical tensile stress due to bending occur at inner fiber:

$$\sigma_{bi}=\frac{Mc_i}{Aer_i}=\frac{Pr_c c_i}{Aer_i}=\frac{P\times(r_i+R)\times\left\{\frac{R^2}{2\left[(r_i+R)-\sqrt{(r_i+R)^2-R^2}\right]}-r_i\right\}}{\pi R^2\times\left\{(r_i+R)-\frac{R^2}{2\left[(r_i+R)-\sqrt{(r_i+R)^2-R^2}\right]}\right\}\times r_i}$$

Using the principle of superposition: $\sigma_t+\sigma_{bi}=\sigma_{max}$ or

$$\frac{P}{\pi R^2}+\frac{P\times(r_i+R)\times\left\{\frac{R^2}{2\left[(r_i+R)-\sqrt{(r_i+R)^2-R^2}\right]}-r_i\right\}}{\pi R^2\times\left\{(r_i+R)-\frac{R^2}{2\left[(r_i+R)-\sqrt{(r_i+R)^2-R^2}\right]}\right\}\times r_i}=\frac{(315\text{ MPa})}{3.5}$$

Solving for equation above yields that

$$R=29.8\text{ mm}$$

4.3.2 Hook Deflection Analysis

I can use Castigliano's theorem to determine the vertical deflection of the hook as shown below:

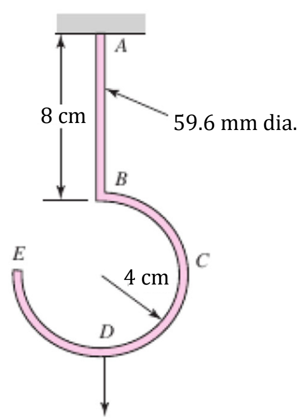

$$U=\int_0^L\frac{F^2}{2AE}dx+\int_0^\pi\frac{M^2R}{2EI}d\theta$$

Therefore, the vertical deflection of the hook is equal to

$$\delta = \frac{\partial U}{\partial F} = \int_0^L \frac{F\frac{\partial F}{\partial F}}{AE}dx + \int_0^\pi \frac{M\frac{\partial M}{\partial F}R}{EI}d\theta = \int_0^L \frac{F\frac{\partial F}{\partial F}}{AE}dx + \int_0^\pi \frac{FR\sin\theta\, R\sin\theta\, R}{EI}d\theta$$

$$= \int_0^L \frac{F}{AE}dx + \int_0^\pi \frac{FR^3\sin^2\theta}{EI}d\theta = \int_0^L \frac{F}{AE}dx + \int_0^\pi \frac{FR^3(1-\cos 2\theta)}{2EI}d\theta$$

$$= \int_0^L \frac{F}{AE}dx + \int_0^\pi \frac{FR^3}{2EI}d\theta - \int_0^\pi \frac{FR^3\cos 2\theta}{2EI}d\theta = \frac{FL}{AE} + \frac{\pi FR^3}{2EI}$$

$$= \frac{(4000\ \mathrm{N})\times(8\ \mathrm{cm})}{\frac{\pi(20\ \mathrm{mm})^2}{4}\times(210\ \mathrm{GPa})} + \frac{\pi\times(4000\ \mathrm{N})\times\left(\frac{8\ \mathrm{cm}}{2}\right)^3}{2\times(210\ \mathrm{GPa})\times\frac{\pi(20\ \mathrm{mm})^4}{64}}$$

$$= 2.4866\times10^{-4}\ \mathrm{m}$$

Therefore, the vertical deflection is pretty small.

The vertical deflection is shown in figure below:

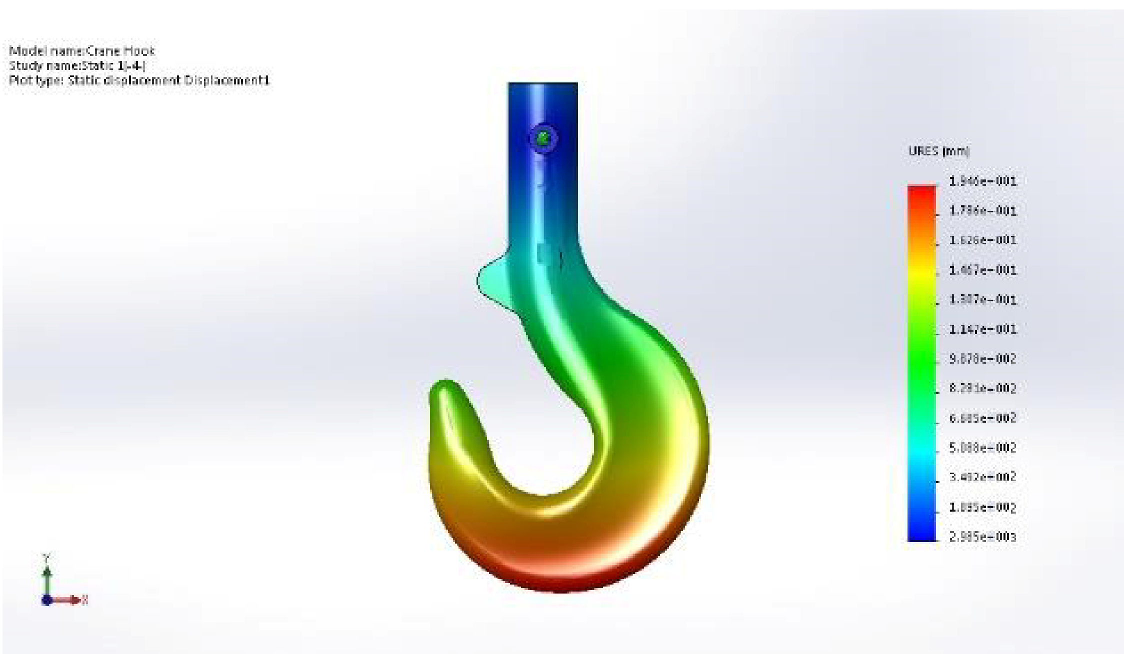

FIGURE 53 VERTICAL DEFLECTION OF THE HOOK

4.4 Cable Analysis

High-carbon steel wires are used for the floor crane. The carbon content is generally 0.70~0.82%.

The minimum diameter of the steel wires can be determined by following:

$$\frac{P}{A} = \frac{\sigma_y}{FS}$$

$$\frac{4000\ \mathrm{N}}{\frac{\pi d^2}{4}} = \frac{520\ \mathrm{MPa}}{3.5}$$

$$\Longrightarrow d = 5.85 \times 10^{-3}\ \mathrm{m} = 5.85\ \mathrm{mm}$$

Therefore, I choose high-carbon steel wires as cable, whose diameter is $5.85\ \mathrm{mm}$.

5 Evaluation of Cost

5.1 Cost of Rectangular Tube

From the website named Midwest Steel Supply, I can know that the prices for the ASTM A500, Grade B steel rectangular tube shown in figure below is $\$465$ per ton. [2]

FIGURE 54 RECTANGULAR TUBE

And the total mass of my final design is equal to 228.68 kg. Therefore, in my final design, the cost for the rectangular tube is equal to

$$\$465\ /\mathrm{ton} \times 228.68\ \mathrm{kg} = \$106$$

5.2 Cost of Hook

From the Amazon, I can know that the price for the hook shown in figure below is equal to $\$51.73$. [3]

FIGURE 55 HOOK

5.3 Cost of Wheels

From the Amazon, I can know that the price for four wheels shown in figure below is equal to $\$24.99$. [4]

FIGURE 56 WHEELS

5.4 Cost of Pulleys and Cable

From the Amazon, I can know that the price for two pulleys and cable shown in figure below is equal to $17.99. [5]

FIGURE 57 PULLEYS AND ROPE

5.5 Total Cost

TABLE 23 TOTAL COST

Items	Prices
Rectangular Tube	$106
Hook	$51.73
Wheels	$24.99
Pulley and Cable	$17.99
Total	$200

From the calculation above, I can know that the total cost of my final design of the floor crane is equal to $\$200$. And compared with the price of the floor crane on Amazon, where I learn that the price for a typical floor crane is almost $\$200$ [6], my cost is reasonable.

6 Conclusion

The aim of my project is to build a fully functional floor crane mechanism which is capable of lifting load up to $400\ \mathrm{kg}$ with the hook and pulley system attached to the horizontal arm. I accurately achieved my goal of lifting the load up and down.

I feel that my design and fabrication was a great success both in terms of strength and stiffness.

The components in the floor crane are:

1. Horizontal Arm: 1 piece, a $100 \times 100 \times 10\ \mathrm{mm}$ square structural tube, A500 steel, $1200\ \mathrm{mm}$ long.
2. Vertical Column: 1 piece, a $150 \times 150 \times 10\ \mathrm{mm}$ square structural tube, A500 steel, $1600\ \mathrm{mm}$ long.
3. Torsion Member: 1 piece, a $100 \times 150 \times 10\ \mathrm{mm}$ rectangular structural tube, A500 steel, $1000\ \mathrm{mm}$ long.
4. Leg Beams: 2 piece, a $100 \times 100 \times 10\ \mathrm{mm}$ square structural tube, A500 steel, $1600\ \mathrm{mm}$ long.

Reference

[1] "Ancient Crane." *GeneratePress*, 8 Apr. 2020, https://www.gruasyaparejos.com/en/construction-crane/ancient-crane/, accessed 20 Nov. 2020.
[2] "Hot Roll Steel Rectangular Tube." *Midwest Steel Supply*, https://www.midweststeelsupply.com/store/hotrollsteelrectangulartube, accessed 20 Nov. 2020.
[3] "Indusco 47400827 Grade 80 Drop Forged Steel Swivel Self-Locking Hook, Painted Finish, 3/8" Trade, 7100 lbs Working Load Limit." *Amazon*, https://www.amazon.com/Indusco-47400827-Self-Locking-Painted-Working/dp/B00CFU3MC6/ref=sr_1_2?dchild=1&keywords=Crane+hook&qid=1606981908&sr=8-2, accessed 20 Nov. 2020.
[4] "Online Best Service 4 Pack Large Steel Swivel Caster Wheel Heavy Duty 3.5" Wheel (3.5" No Brake)." *Amazon*, https://www.amazon.com/Large-Steel-Swivel-Caster-Wheel/dp/B00HQI88I0/ref=sr_1_13?dchild=1&keywords=Crane+wheel&qid=1606982353&sr=8-13, accessed 20 Nov. 2020.
[5] "Artilife M50 Single Crane Pulley Block Stainless Steel 304 Lifting Crane Swivel Hook and 10M High Strength Nylon Pulley Rope & Connection Buckle." *Amazon*, https://www.amazon.com/Artilife-Stainless-Lifting-Strength-Connection/dp/B08CH35VHF/ref=sr_1_13?dchild=1&keywords=Crane+pulley&qid=1606982505&sr=8-13, accessed 20 Nov. 2020.
[6] "OTC 1820 4400 lb. Max Capacity Heavy-Duty, Folding Shop Crane." *Amazon*, https://www.amazon.com/OTC-1820-Capacity-Heavy-Duty-Crane/dp/B000HTAKXQ/ref=sr_1_3?dchild=1&keywords=Floor+Crane&qid=1606983092&sr=8-3, accessed 20 Nov. 2020.
[7] Deborah L Boklund Moran, "Hook Assembly and Kit," United States Patent, Patent No.: US 20060289714 A1.
[8] John Joseph Rinaldo, "Pot Rack Hook," United States Patent, Patent No.: US 20120199714 A1.
[9] Dominique Rouzaud, "Safety Locking Device Having a Rocking Hook," United States Patent, Patent No.: US 005257840 A1.
[10] Ralf Esising, Gersemsky, Lichtenvort, Walloschek, "Load Hook," United States Patent, Patent No.: US 20070176446 Al.
[11] Ralf Esising, Gersemsky, Lichtenvort, Walloschek, "Load Hook," United States Patent, Patent No.: US 007607707 B2
[12] "Types of Bearings - A Thomas Buying Guide." *THOMAS*, https://www.thomasnet.com/articles/machinery-tools-supplies/bearing-types/, accessed 20 Nov. 2020.
[13] "Metals and Alloys – Densities." *The Engineering Toolbox*, engineeringtoolbox.com/metal-alloys-densities-d_50.html, accessed 20 Nov. 2020.

Christopher King